SSC-111

PRELIMINARY STUDIES OF BRITTLE FRACTURE PROPAGATION IN STRUCTURAL STEEL

by

W. J. Hall
W. G. Godden
and
O. A. Fettahlioglu

SHIP STRUCTURE COMMITTEE

Serial No. SSC-111

First Progress Report
of
Project SR-137

to the

SHIP STRUCTURE COMMITTEE

on

PRELIMINARY STUDIES OF BRITTLE FRACTURE PROPAGATION IN STRUCTURAL STEEL

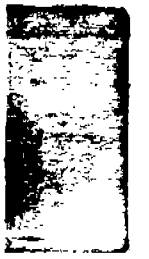

by

W. J. Hall, W. G. Godden and O. A. Fettahlioglu

University of Illinois
Urbana, Illinois

under

Department of the Navy
Bureau of Ships Contract NObs-65790
BuShips Index No. NS-731-034

transmitted through

Committee on Ship Structural Design
Division of Engineering and Industrial Research
National Academy of Sciences-National Research Council

under

Department of the Navy
Bureau of Ships Contract NObs-72046
BuShips Index No. NS-731-036

Washington, D. C.
National Academy of Sciences-National Research Council
May 15, 1958

PRELIMINARY STUDIES OF BRITTLE FRACTURE PROPAGATION IN STRUCTURAL STEEL

ABSTRACT

This report describes the initial research work on a program concerned with a study of the propagation of brittle fractures in wide steel plates. The tests are being conducted to obtain information concerning the crack speed and the strain distribution in a mild steel plate during brittle crack propagation.

The development work involved consideration of (a) two methods of crack initiation, (b) instrumentation, (c) methods of specimen cooling, and (d) specimen geometry. The adopted specimen consists of an insert plate welded to pull plates mounted in the testing machine. The test procedure consists of cooling the plate with dry ice, loading to the desired average stress level, and initiating the fracture by means of an impact that drives a wedge into a notch in the edge of the specimen. Strain and speed measurements are recorded by means of cathode-ray oscilloscope recording equipment.

After the development work had proceeded to the point where the test procedure was fairly reliable, a preliminary program of tests of 2-ft wide rimmed steel plate specimens was undertaken. The more important observations resulting from these tests may be summarized as follows: (1) crack speeds ranging from 1150 to 5900 fps were recorded, (2) absolute peak elastic strains as high as 0.002500 in. per in. were recorded in the vicinity of the fracture with negligible permanent set remaining after the fracture; (3) as the distance between a vertically oriented strain gage and the fracture path increased, the magnitude of the strain pulse decreased and the pulse time increased.

TABLE OF CONTENTS

PRELIMINARY STUDIES OF BRITTLE FRACTURE PROPAGATION IN STRUCTURAL STEEL

I. INTRODUCTION

1. General

Perhaps the most important and desirable mechanical property of structural steel, under normal loading conditions, is its ability to undergo considerable deformation with large energy absorption before failure. However, under certain conditions of stress, temperature, and geometry, it may fracture in a brittle manner; this type of fracture is characterized by a small amount of deformation and a corresponding small amount of energy absorption. During the past half century many structural failures exhibiting brittle fractures have been reported in the literature. These failures have occurred in a variety of structures, including ships, oil storage tanks, pressure vessels, and bridges. However, not until World War II--when the failures of a large number of steel merchant ships attracted public attention--did the problem of brittle fracture of steel receive the serious attention it deserved.

As a result of extensive research since World War II, the probability of brittle failure in many applications today can be minimized by giving proper attention to such variables as type of material, geometry, method and sequence of fabrication, temperature, and stress level. Also, in selected applications, it is now possible to effectively use crack arrestors, which may stop the propagation of brittle fractures. In spite of these marked advances, a clear understanding of the brittle fracture mechanism is still needed for the eventual development of satisfactory design procedures.

2. Object and Scope of Investigation

This report describes the initial phases of a fundamental investigation of brittle fracture mechanics. The object of the investigation, which began in July

1954, is to study the propagation of brittle fractures in wide steel plates. Eventually, it is hoped that as a result of these studies it will be possible to develop hypotheses that can be used to verify and predict the behavior of steel when it fractures in a brittle manner.

The first task of the program was to decide what should be measured and in what manner it might be accomplished. After a thorough study of the problem, it was decided that an investigation should be made of the crack speed and the change in strain distribution in the plate while the fracture is propagating. Little of the brittle fracture work reported previously has included the results of high-speed measurements made during the propagation of brittle fractures.

The initial phase of this investigation consisted of development work and was a joint effort with another related program concerned with the evaluation of crack arrestors (Ship Structure Committee Project SR-134). However, only that development work which relates directly to the objectives of the fracture mechanics program is described in this report.

Four items that required early consideration were (a) crack initiation, (b) specimen cooling, (c) instrumentation, and (d) specimen geometry. Two general methods of crack initiation were investigated. One involved an explosive device (the powder-detonator bolt) and the other involved the notch-wedge-impact system, a method similar to that developed by other investigators. Since at the beginning of the program it was decided that crushed dry ice could be used as the cooling agent, the development work consisted of devising appropriate containers and improving the efficiency of the cooling systems employed. The instrumentation problems included the selection and development of such things as pickups, wiring, recording instrumentation, data reduction, and required more effort than any other phase in the early stages of the program. Except for the powder-detonator bolt tests, which utilized relatively small-scale specimens, most of the development work was performed with flat plate specimens 3/4 in. thick by 2-ft wide by 6-ft

long (clear distance between pullheads). For the most part, only the significant details of the development work are presented in this report. In general, the final successful arrangement or method is described. However, in some cases it was felt desirable to describe briefly some of the unsuccessful items of development in the hopes that this would be of aid to investigators on related future programs.

After the development had proceeded to the point where the test procedure was fairly reliable, a program of tests of 2-ft wide specimens was undertaken. The purpose of this series of tests was threefold: first, to obtain measurements of the speed of crack propagation and a measure of the strain pattern in the vicinity of the running crack, as well as at other selected points; second, to check on the consistency of these data by a series of duplicate tests; and third, to develop a procedure satisfactory for testing 6-ft wide plate specimens. Part III of this report contains a description of the tests of the 2-ft wide specimens and the resulting data.

3. Brief Reference to Published Work

The first wide-plate tests conducted at the University of Illinois involved static tests of internally notched steel plates of various widths to determine the relation between the behavior of wide plates and the mechanical properties of the material.[1]

The present University of Illinois program involves tests of wide plates that are instrumented to obtain measurements of crack speed and strain response as the crack propagates. The fracture is initiated from edge notches by means of a wedge with external impact. In addition to the material presented here, reports are available on some of the other work accomplished as a part of this program.[2, 3]

The method of testing used is similar to that used by Robertson in England,[4] and Feely and associates in the United States.[5, 6] Reports are also available

on other experimental work that is related directly or indirectly to the work reported here, [7--13] as is material presenting the theoretical aspects of the b ittle fracture mechanics problem.[12--16] "The Velocity of Brittle Fracture," by Roberts and Wells, a summary of brittle fracture speed measurements in steel as reported in published works, is of particular interest with respect to the speed measurements undertaken as a part of this investigation.[13] This paper reports measurements made by several different methods on various types and sizes of steel specimens and showed speeds in the range of 3370 to 6600 fps.

The above references comprise only a small part of the available literature in the brittle fracture field. Other important work in this field may be traced through the extensive bibliographies contained in each of the references cited.

4. Acknowledgment

The work described in this report was conducted in the Structural Research Laboratory of the Department of Civil Engineering, University of Illinois, and the program is sponsored by the Ship Structure Committee. The members of the Brittle Fracture Mechanics Advisory Committee, under the cognizance of the Committee on Ship Structural Design of the National Academy of Sciences-National Research Council, have acted in an advisory capacity in the planning of this program.

The project is under the general direction of N. M. Newmark, Professor and Head of the Department of Civil Engineering. The authors wish to thank Dr. Newmark, W. H. Munse, Research Professor of Civil Engineering, R. J. Mosborg, Assistant Professor of Civil Engineering (Supervisor of Project SR-134, "Crack Arrestors,") and V. J. McDonald, Research Assistant Professor of Civil Engineering (in charge of instrumentation) for their helpful advice and assistance. The writers also wish to acknowledge T. J. Hall, R. Lazar, T. M. Lynam, K. Hayashi, and particularly S. T. Rolfe, Research Assistants in Civil Engineering, and D. F. Lange, Shop Foreman, for their assistance with the laboratory work.

The powder-detonator bolt development work was done by Dr. W. G. Godden, Lecturer, Queens University, Belfast, Ireland, while he was associated with the Structural Laboratory at the University of Illinois in 1954-55. That portion of the report dealing with the program of tests of the 2-ft wide plate specimens was drawn from a Master of Science dissertation submitted to the Graduate College of the University of Illinois in 1956 by Mr. O. A. Fettahlioglu.[17]

II. INITIAL DEVELOPMENT WORK

5. Fracture Initiation Studies

Two general methods of fracture initiation, one employing an explosive and the other employing a notch, a wedge and external impact, were investigated early in the program. Both methods involve a high rate of local straining, commonly recognized to be one of the factors that may contribute to the initiation of brittle fracture in steel.

(a) Powder-Detonator Bolt

Development of the powder-detonator bolt was undertaken because it was believed possible to initiate a brittle fracture by exploding a charge within a sealed detonation chamber located at a stress raiser in the specimen. The advantages of simplicity, compactness, and utility at any location on the specimen made this method of initiation particularly attractive. However, two of the major problems encountered in the development of such a device were (a) sealing the chamber against pressure leakage and (b) protecting the charge from condensation of water, particularly at low temperatures.

The body of the device consisted of a high tensile bolt that was bored to hold an explosive charge. The bolt was designed to fit closely in a notched hole in a specimen and was sealed at the ends of the notched hole so that the pressure from the blast would emit only radially from orifices in the bolt shank

to produce a pressure impulse in the stress raiser. Black powder was used as the explosive medium because it reaches a ceiling pressure of about 20,000 psi after which burning ceases. It is estimated that the maximum pressure is obtained in four to five milliseconds when the finest (FFFg) commercially available grain size of powder is used. The explosive was detonated electrically with a model airplane-type glow plug packed with finely ground black powder dust. The priming mechanism required a pressure valve between the main charge and the glow plug to prevent blowout of the glow plug.

The most serious problem encountered in the development of the detonator bolt was sealing against pressure leakage at the bolt-plate junction. Recesses were machined to receive solder-sealing gaskets which were held in place by the shoulder of the bolt. This method of sealing was satisfactory provided there was no excessive yielding in the vicinity of the hole near the plate surfaces.

After being assembled, the bolt was kept in a desiccator until it was required for the test. A specimen with the powder-detonator bolt in place is shown in Fig. 1; details of the detonator bolt are shown in Figs. 2 and 3.

In the test specimens, the detonator bolt was fitted into either a 5/8-in. diameter drilled hole with two diametrically opposite 1/16-in. deep jeweler's saw-cut stress raisers transverse to the direction of applied stress, or a 5/8-in. diameter punched hole. In the former case, the depth of the sawed notches was limited by the gas-sealing arrangement. The punched hole was tried because of the known susceptibility of sheared edges to brittle fracture. Details of these stress raisers are presented in Fig. 4.

Because the detonator bolt device failed to initiate even one fracture in these exploratory tests, the results are summarized only briefly in Table 1. The details and dimensions of the specimens used in connection with the detonator bolt tests are shown in Figs. 5 and 6, with additional explanation presented in Table 1. The 12-in. wide specimens were welded to pull plates for testing. The material was a rimmed

steel, (Steel E, Plates 16-1 and 17-A) having yield and maximum strength values of about 31,000 and 63,000 psi respectively, and a Charpy V-notch 20 ft-lb value of about 70 F. The check analyses and mechanical properties of the steel are summarized in Tables 2 and 3, and in Fig. 10.

As noted in Table 1, the detonator bolt was tried with each size of specimen and with each type of stress raiser. At the time the detonator device was fired, the static stress on the net section of the specimens was in the range of 30,000 to 35,800 psi, and the temperature was in the range of 5 to 20 F. There was no sign of fracture initiation in any of the tests. Unburned powder in the bolt in many of the tests indicated that the maximum pressure had been obtained. The detonation generally produced extensive yield patterns in the vicinity of the stress raisers; these yield patterns could be seen clearly on the polished surfaces. Measurements of the enlargement of the diameters of the stress-raiser holes are noted in Table 1 and amounted to as much as 0.015 in.

Test 8-DB (Table 1), a static tension test, was made to ascertain the approximate fracture strength of the test pieces that had been used with the powder detonator bolt. The fracture originated at the punched hole (Fig. 8) at an average stress of 42,700 psi. One static test (Test 9-DB, Fig. 7) of an eccentrically loaded specimen, having a semicircular punched notch as a stress raiser, was made to investigate any possible stress correlation with the previous tests. After considerable yielding, the specimen failed at an average net stress only slightly higher (44,900 psi) than that found in Test 8-DB noted above. The fractured specimen is shown in Fig. 9.

Several additional tests (6-DB and 7-DB) of the 12-in. specimens were made using the detonator bolt as a static pressuring device. With an average net stress of 30,000 psi and application of an additional hydraulic pressure of 33,000 psi to the bolt, the only visible results were an enlargement of the hole and extensive yield patterns on the polished surface.

Although the exact reason for the failure of the detonator bolt device to initiate any fractures is not precisely known, one possible reason is that the amount and rate of loading, resulting from the explosion, may not have been quite high enough. As a result of the above tests, the detonator bolt scheme of initiating fractures was dropped from further consideration as a part of this program.

(b) Notch-Wedge-Impact Method

The second method of fracture initiation, hereafter called the notch-wedge-impact method, has been used in various forms for fracture initiation since the beginning of the program. To supply the external impact, a gas-operated piston device capable of providing up to 3,000 ft-lb of external energy was developed. The details of this device are presented in Figs. 11 and 12. Bottled commercial nitrogen gas was used as the pressurizing medium. The gas pressure and piston stroke could be altered to produce the desired energy output. The piston, mechanically restrained during the pressurizing and manually released at the time of firing, drives a wedge into a prepared saw-cut notch in the edge of the plate specimen. To absorb the reaction of the piston device during acceleration of the piston, the device was tied to a weight (approximately 120 lb) which bore against the far side of the specimen at the notch line. The term "notch line" refers to an imaginary horizontal line (when the plate is held vertically in the testing machine) that connects notches that had been made previously on both edges of the plate.

The apparatus that supported the impact device and reaction weight was attached to the top pullhead and thus was semi-isolated from the specimen. The apparatus was also tied back to the columns of the machine with wires to minimize the movement of the system when the firing latch was tripped.

A summary of the early development tests of 2-ft wide plane plate specimens is presented in Table 4. (The original testing arrangement may be seen

in Figs. 14, 15, and 18.) These specimens were used for the development and evaluation of the notch-wedge-impact method of fracture initiation, for the cooling apparatus, the support apparatus for the gun and weight, and for the trials of the various types of recording instrumentation and associated pickups.

Specimen A-1 was cut from a 3/4-in. plate of A-285 Firebox-Grade C steel. The test piece was 2-ft by 6-ft in plan dimension and was welded to the pullheads of the 600,000 lb screw-type testing machine. After this specimen was tested, a central 18-in. portion, which included the fracture, was cut out; the remaining end pieces, welded to the pullheads, were used for the pull plates in future 2-ft wide tests. All subsequent 2-ft wide specimens consisted of 3/4- by 24- by 18-in. plate inserts, welded to the pull plates, to give an over-all plate specimen 2-ft by 6-ft in plan dimension. This small-scale specimen was geometrically similar in plan dimensions to the 6-ft wide plate specimens used for the later tests (6-ft wide by 18-ft long); in each case, the length was the clear distance between edges of the pullheads. All of the specimens were oriented with the direction of rolling parallel to the long axis of the specimen and perpendicular to the direction of crack initiation. The plate numbers of these inserts are listed in Table 4 and, with the exception of Specimen A-1, the check analyses and mechanical properties of the steels are presented in Tables 2 and 3, and Fig. 10.

Several notch and wedge details were used in the various tests. In Specimen A-1, a tapered circular wedge was driven broadside into a tapered hole near one edge of the plate (see Table 4, and Figs. 13(a) and 14). The broadside wedging scheme was abandoned because of the torsional vibration which was evident in the recorded data. Edge-on wedging was adopted beginning with Specimen E-1. The details of the various types of notches and wedges are noted in Table 4 and Fig. 13.

As a result of the foregoing development work, the notch-wedge configuration shown in Fig. 13(c) was adopted. This method of initiation is an outgrowth of a method used by Robertson in England[4] and is similar in many respects to that used by the Standard Oil Development Company in their tests.[5, 6] A theoretical impact of about 1200 ft-lb was established as sufficient to insure fracture initiation for the particular material and test conditions under consideration.

Some of the details of the fractures resulting from the tests summarized in Table 4 are shown in Figs. 14--17. The term "submerged crack," as used in Table 4, denotes a relatively short, wedge-driven crack that propagates only a few inches but does not cleave through the plate surface completely. It is characterized by a depression on the plate surface, which normally corresponds to a reduction in the plate's thickness of about 1 to 2 per cent. The internal surfaces of the submerged cracks shown in Fig. 17 were revealed by cutting out the notch region after the test and pulling the pieces apart statically. In this figure, the S (South) and N (North) letters in the specimen designations refer to the original plate orientation in the testing machine. The two submerged cracks for Specimen E-3 are found in the top half of the plate as indicated in Table 4. The extent of penetration of the original submerged crack is indicated by arrows in the figure.

In the case of Specimen E-11, a series of residual strain measurements was made along the notch line to study the effect of welding the insert to the pull plates. The welding produced tensile residual strains of 125 micro in./in. in the longitudinal direction of the specimen at the notch line.

6. Cooling Apparatus

Since the beginning of the program, crushed dry ice has been used as the cooling medium. In the early tests, the dry ice was placed in wire baskets, which in turn were held in trays as indicated in Fig. 15; the specimen was then wrapped with insulation material and cloth as shown in Fig. 18. Later, a much more efficient wood and screen box was prepared to hold the dry ice. These boxes are described in Section 9 of this report.

7. Speed Detectors and Recording Instrumentation

In order to obtain a measure of the crack speed, it appeared that the best available method would consist of placing detectors (conducting strips or wires mounted perpendicular to the expected crack path) on the surface of the specimen. The breaking of the detectors would be monitored on a recording instrument to obtain a measure of the time required for the crack to propagate from one detector to the next. With a knowledge of the time of breaking and the distance between the detectors, the crack speed could be computed. As conductors, lamp black, fine powdered aluminum, pulverized charcoal, graphite, brittle copper wire, extruded bismuth wire and silver-printed circuits were tried. Stresscoat, shellac, Duco cement, and several commercial electronic insulating substances were tried as insulation and gluing bases. After considerable investigation, the two most promising types of crack speed detectors were found to be extruded bismuth wire (ranging from 0.006 in. to 0.012 in. in diameter), glued to charred sulphide paper with Duco cement, and silver circuits, printed on sulphide paper and then charred. Each of these detectors was glued to the surface of the specimen with Duco cement.

One of the biggest questions in connection with the use of such devices was the consistency of the detectors, i.e., did all the detectors break at the same strain? An attempt was made to obtain some measure of the consistency of the detectors by gluing a number of them to steel beam specimens, which in turn were placed in a rapid-loading device available in the laboratory. This device is capable of attaining a maximum load of 20 kips in 2 to 3 milliseconds. One of the beam specimens with detectors attached is shown mounted in the pulse loading machine in Fig. 19. After examining the records from these tests, it became apparent that slight eccentricities of loading, or unevenness of loading, could cause quite a variation in strain at the detector. Thus it was established that this was not a fair measure of the consistency of the detectors. Also, the

loading rate in these tests, on the order of 2 to 3 milliseconds, is considerably slower than the loading rate in the brittle fracture process.

Later in the program, Baldwin SR-4 Type A-9 strain gages (single-wire, 6-in. gage length) were used for crack speed detectors. Although they are somewhat more ductile than the other detectors, it was felt that the greater ease of application and smaller variation of dimensions and properties of these strain gages made their use more desirable.

Early in the program, a comparison was made on Specimen A-1 of the strain response as recorded on an oscillograph and an oscilloscope. In these exploratory tests, it was observed that the oscillograph did not have a frequency response great enough to provide accurate strain records; thereafter, oscilloscopes were used exclusively to record strain. In the test of Specimen E-11, the strains were recorded on a DuMont dual-beam oscilloscope and photographed with a DuMont 35-mm strip-film camera running at its fastest speed (10,800 in./min). Even at this speed, however, the record was too condensed for satisfactory reading. Thus it was decided that future recording would require that the traces should sweep the scope face (time-wise) and be photographed on still film. However, the data from the test of Specimen E-11 were of considerable value in that the record showed crack speeds ranging from 1600 to 2700 fps, with speed increasing in magnitude as the crack progressed across the specimen.

The test of Specimen E-10 resulted in a 3-in. submerged crack as noted in Table 4. In this instance, the partial fracture broke the trigger wire, energized all of the circuits, and provided a strain record of unusual interest. The test data indicated that, in the immediate vicinity of the notch, sizeable strains could be expected; at distances relatively far from the crack, the strains were affected to a minor extent by the wedging force. This was the first definite indication that the notch-wedge-impact method of fracture initiation produced a much smaller strain response at some distance from the notch than would occur as a result of a

propagating crack in a complete fracture test. This same conclusion has been reached in connection with similar studies on 6-ft wide plates.[3]

III. PRELIMINARY TEST SERIES--TWO-FOOT WIDE SPECIMENS

8. Specimen Material and Preparation

Lukens rimmed steel (Heat No. 16445; Laboratory designation Z1A, i.e., Steel Z, Plate 1A) was used for all of the specimens of the preliminary series of tests. The check analysis of this steel is presented in Table 2, tensile-test data in Table 3, and the Charpy V-notch results in Fig. 10. The V-notch in the Charpy specimen was oriented perpendicular to the plate surface, and the test bar was aligned parallel to the direction of rolling. This material had a Charpy V-notch 20 ft-lb value of about 70 F, which made it a desirable material for the particular type of test used in this investigation.

The ten Z1A series specimens (3/4-in. thick by 24-in. wide by 18-in. deep inserts) were cut from a 6-ft by 9-ft plate as shown in Fig. 20. As may be noted in this figure, the direction of rolling was in line with the vertical axis of the specimen, i.e., always perpendicular to the notch line. All specimens were prepared with two notches, one on each edge of the specimen, to provide a symmetrical specimen; the notch details are described in Section 5(b) of this report. The one-inch notch on each edge of the specimen resulted in a net section 22 in. by 3/4 in.

9. Test Apparatus

The tests of this investigation were performed in a 600,000-lb screw-type testing machine. A typical test setup with all apparatus in place is shown in Fig. 21.

The brittle fracture was initiated at the notch by driving a tapered cold-chisel wedge (approximately 16° included angle, 5 1/2 in. long and weighing 1 lb) into the notch by means of the gas-operated piston device. The specimen

was cooled with crushed dry ice, held in containers fitted against each side of the specimen. A container is shown mounted in place on a specimen in Fig. 21 and is shown separately in Fig. 22. The central portion of the box was recessed to keep the dry ice from contacting the instrumentation in the vicinity of the notch line. This extremely efficient arrangement cooled the specimens from room temperature to approximately 0°F in about one hour.

10. Instrumentation

(a) General

All specimens of this series, with the exception of Test 1, were instrumented in essentially the same manner and with essentially the same equipment. The variation between specimens occurred in the specific number of channels allocated to strain measurements and to crack speed measurements. The instrumentation and recording equipment will be discussed in general terms; the reader is directed to the actual records for the specific arrangements for a given test.

(b) Strain Gages, Speed Detectors, Triggers and Thermocouples.

Baldwin SR-4 Type A-1 strain gages (13/16-in. gage length) were used for Tests 1, 5, 6, 7 and 8, and Baldwin SR-4 Type A-7 strain gages (1/4-in. gage length) were used for Tests 9, 10 and 11. The active strain gages, as contrasted to those used only for static monitoring purposes, are hereafter commonly referred to as dynamic strain gages. These dynamic strain gages form a part of a circuit connected to an oscilloscope during the fracture propagation. When this preliminary series of tests was started, three types of speed detectors were being utilized: (1) single-wire SR-4 Type A-9 strain gages (6 in. gage length), (2) single-wire silver-printed paper strips (charred), and (3) small-diameter extruded bismuth wire. All of these, with suitable insulation and lead attachments), were cemented to the specimen with a thin layer of Duco cement. As the testing on the various phases of the program progressed, it became apparent that the Type A-9 strain gages were the easiest to install and seemed to provide results as consistent as the other types. Beginning with Test 9, these

Type A-9 strain gage detectors were used exclusively for speed detectors, while silver-printed detectors were used exclusively for triggering the instrumentation. Typical examples of specimens with the various types of instrumentation are shown in Figs. 23--25.

Some difficulty was experienced in obtaining reliable static strain readings during cooling, until it was realized that an equal length of lead wire for each gage must be placed in the cooled region. This applied to compensating gages as well as active strain gages. After the lead wire lengths were properly adjusted, the discrepancy in strain readings between those taken at room temperature and during cooling was almost negligible.

All of the instrumentation on the specimen was covered with a plastic curtain before cooling to minimize the amount of condensation forming on the gages and wiring and to prevent stray pieces of dry ice from grounding the gages. Copper-constantan thermocouples were used to measure temperature, and the temperature readings were recorded automatically on a Micromax strip-chart recorder during the cooling process.

(c) Recording Equipment

At the time these specimens were tested, a maximum of five channels of high-speed cathode-ray oscilloscope equipment was available for recording. This equipment consisted of two dual-beam cathode-ray oscilloscopes (DuMont types 322 and 322a), modified to provide greater sensitivity, and one Tektronix type 512 oscilloscope driven by a Tektronix Model 122 preamplifier. The recording instrumentation is shown in Fig. 26.

All traces were recorded photographically as a function of a common time base supplied from the Tektronix oscilloscope. This same electronic sweep generator provided the desired blanking and intensifying signals to minimize fogging of the record before and after the test period.

The four DuMont channels were optically combined and superimposed on a single frame in the interests of maximum photographic definition. The cameras used were the DuMont 321, which served as a single frame camera for the four DuMont channels, and a 35-mm Exacta V, used for the Tektronix unit. The recording equipment is shown in block diagram form in Fig. 27.

The DuMont 322 sensitivity was sufficient to allow about 1-1/2 in. of trace deflection for 1000 micro in./in. strain; the 322a sensitivity was less than this with 1000 micro in./in. strain deflecting the trace about 1/2 in. Whenever possible, the 322a traces were used to record the highest magnitudes or signals (described in Section 10d) other than strains. The frequency response of both units was flat within 5 per cent from zero to 100 kc and down not more than 50 per cent at 300 kc. Since the majority of records taken were of the order of two or more milliseconds sweep time, and the recorded signals did not approximate step functions, the latter response was considered adequate.

The frequency response of the Tektronix 512 unit operating off the Model 122 preamplifier was essentially limited by the characteristics of the preamplifier. This amplifier has a bandwidth of 0.2 cps to 40,000 cps. Care was taken to insure recording of signals whose shapes could be passed within this band, and all records were checked to make sure that recorded rise times did not closely approach this upper limit. The sensitivity of the combination was more than adequate for these tests, although the low frequency cutoff did affect the calibration procedure.

(d) Input Circuits

The signals fed to the recording equipment consisted of a sweep-triggering pulse, strain signals and crack detector signals. These were used respectively to start the recording equipment, to provide a series of strain signals that were recorded as strain-time curves, and to time the breaking of the crack detectors. In the case of the latter signal, the detectors opened an electrical circuit as they broke and fed step voltages to the recording channel. The amplitudes of the steps were in the ratios of

1, 2, 4, 8 and 16. Thus each step of different magnitude could be identified with the particular detector to which it was connected and allowed positive determination of the sequence of detector failures.

The sweep was triggered when a circuit was opened by the breaking of a trigger detector. This removed a bias signal from a triggering thyratron and allowed it to start conducting. The step voltage, which resulted from the initiation of conduction, was fed into the standard circuits of the Tektronix 512. The thyratron was not added until approximately midway through this series of tests. Its function was to prevent multiple sweeps on the single recorded frame. The multiple sweeps obscured the traces of interest and were triggered by such things as chatter of the initiating wedge and accidental grounding of the trigger remnants. With the thyratron in the circuit, reinitiation could not occur until the thyraton was reset manually.

The strain gages were connected in the customary wheatstone bridge circuit with one active and three dummy gages. These gages were excited by direct current and their outputs fed to the recording channels. The common lead for all the bridges was grounded. Typical input circuits to the recording instrumentation are shown in Fig. 28.

(e) Calibration and Measurement Procedures

Calibration of the strain measuring channels followed the customary procedure of shunting the gages with a resistance whose equivalent strain value is known. Both the active arm and the adjacent dummy gage were shunted successively, giving a tension and a compression calibration. Only one calibration value was used inasmuch as other tests indicated that the linearity of the recording system was adequate within the limit of resolution of the record. The crack detector calibration was obtained by successively opening switches in series with the various detectors and recording the trace steps. These calibration switches and circuits are indicated in Fig. 28.

When the DuMont type-321 camera was used, the film was moved slowly past the lens as the various calibrating switches were operated. This resulted in a calibra-

tion record of the type shown in the lower portion of Fig. 29. A typical test record taken with the DuMont equipment also is shown in the upper portion of Fig. 29.

Because the Tektronix oscilloscope had a low frequency cutoff point and because the Exacta V camera did not permit operation as a strip-film camera, a different calibration technique was used with this unit. A free-running sweep was applied to the scope with the camera shutter open. The calibration resistance was then shunted across the desired gage. The result of the above operation was that the trace remained at "zero" until the resistor was connected and then stepped to a value corresponding to the amount of the calibrating signal. This step decayed exponentially, and successive traces showed this exponential decay as a darkened area on the negative. The actual calibration value is that distance between the zero line and the maximum displacement of the trace. Successive frames were used for tension and compression calibration. The lower and right portion of Fig. 30 illustrates the step and decay phenomenon for the Tektronix unit. The chopped decay actually appears as a solid band as can be seen from the photograph. A typical test record taken with the Tektronix unit also is shown in the upper left portion of Fig. 30.

The time axis was calibrated by putting a time signal of known frequency on all channels simultaneously and photographing one sweep immediately after the test was completed.

All horizontal deflection plates were connected in parallel and were driven from a common amplifier. However, individual construction of the various guns and deflections systems results in slight horizontal displacements between the traces and in slight differences of deflection sensitivity. For these reasons, it was necessary to calibrate all traces with a simultaneous signal. One phase of this operation that may be slightly questioned is the time lag between the actual test and the calibration of the horizontal sweeps. There is a parallel question, of course, in calibrating the vertical system before the test period. However, the question of stability of gain magnitude and trace deflection was studied and considered to be satisfactory on the basis of the

consistency of trace lengths and locations obtained from the various tests in a series of investigations.

(f) Data Reduction

The only features of data reduction in this investigation that may not be standard were the method of tying the various traces together with respect to time and the significance of the time axis values.

In general, some arbitrary point was taken along the sweep length and called "zero time." This may or may not correspond to the earliest point on the recorded traces. The point was usually selected near the early portion of the sweep at the first peak of the time-calibrating sine-wave. This was done to provide a convenient reference point that would be common to all traces. The record was then reduced in the customary manner of reading strains against time, or of noting the times at which the detectors failed. Individual traces were read with individual calibrations on both the time and strain axes. The result is a series of correlated measurements with an arbitrary zero time.

As a result of this procedure, a plot of the reduced data may show values beginning at a negative time. The earliest time noted for any trace (it may be before or after the arbitrarily selected zero time) was some finite but unknown amount of time after the breaking of the sweep triggering wire (approximately 20 microseconds), and was a completely unknown amount of time after the initiating wedge enters the plate. This time has been tacitly assumed small.

In plotting the data for this report, zero time was taken as the earliest recorded time for all traces for a particular test; thus, the zero times noted are arbitrary and are not common to all tests, nor are they related to the time at which the fractures initiate.

11. Test Procedure

The steps involved in performing a test are listed in order as follows:

1. The specimen is preloaded at room temperature and the static strain values are recorded.
2. Dynamic recording instrumentation is connected and checked.
3. Dry ice is placed in the cooling containers and cooling begins.
4. About ten minutes before actual test time (as estimated from the cooling rate), the calibration traces are recorded; the specimen is loaded and static strains are recorded.
5. The gas-operated piston device is pressurized, instrumentation readied, and when the desired temperature is reached, the piston device is fired manually.
6. After the test, the time calibrations are recorded and all strain gages are checked statically while cold, and again after the specimen has warmed to room temperature.

12. Results and Interpretation of Tests

(a) General

A summary of this preliminary series of tests is presented in Table 5. The final test made as a part of the initial development work is listed as Test 1 (Specimen E-18) in this table. It is included with this series of preliminary tests because an excellent record was obtained, and because it was essentially the basis for the Z1A series of tests reported here.

After completion of the development work, it seemed desirable to run a series of tests of 2-ft wide specimens. There were three main reasons for this series: first, to obtain additional measurements of the speed of crack propagation and of the strain pattern at selected points; second, to check on the consistency of the data by running several duplicate tests; and third, to further the development of various items in preparation for the testing of 6-ft wide plate specimens.

As indicated in Table 5, the tests of this particular phase of the program were divided into three groups. The first group (Tests 2--4) was run to investigate the fracture characteristics of the particular steel stock. The results indicated that brittle fractures could be expected to propagate consistently at an average net stress of 18,000 psi, a temperature of about 0°F, and with an external impact of 1200 ft-lb for fracture initiation. These values of stress, impact, and approximate temperature were used for all of the tests of the second and third groups, the instrumentation then being the only variable.

In general, all of the second group of specimens (Tests 5--8) were instrumented in an identical manner, and all of the third group of specimens (Tests 9--11) were likewise instrumented in an identical manner. Exceptions resulted when an additional channel of instrumentation became available and when certain gages failed at the last moment.

The scaled record, instrumentation layout, and position of the fracture for each of the instrumented specimens are presented in Figs. 32 through 39. In these figures, the nomenclature should be self-explanatory, with perhaps the exception of Y_{c-g}, which is the vertical distance from the crack to the gage. All strain diagrams are plotted beginning at the initial test-load strain; thus the strains as shown may be considered to be absolute values. The test-load strain values were obtained for each particular gage during the static pre-loading at room temperature. The crack speeds computed from the detectors are tabulated in Table 6.

Of the seven instrumented specimens, only four provided completely satisfactory records. Considering the stage of development of the work, tests, and instrumentation, however, this situation was believed to be very encouraging.

(b) Test 1 (Specimen E-18)

Specimen E-18 was tested at an average net stress of 25,000 psi, a temperature of 13 F, and with an external impact of 1200 ft-lb for fracture initiation. A print of the actual test record is shown in Fig. 31, and the scaled record, instrumentation layout, and position of fracture are presented in Fig. 32. The speed detectors indicated crack speeds of 2400 to 4200 fps, as noted in Table 6. The two vertically oriented strain gages (Fig. 32) showed absolute peak strains of about 1750 and 2500 micro in./in. respectively, followed by a rapid drop to absolute zero. No measurable permanent set in the strains was evident.

(c) First Group (Tests 2, 3 and 4)

The first three specimens of the ZIA series were tested without any instrumentation. The purpose of the tests was to find a combination of stress, temperature, and impact that would insure the propagation of the brittle fracture across the 2-ft wide plate. This group of tests was necessary since plates from this particular heat of steel had not been used previously.

It appeared desirable on the basis of previous work to maintain the impact energy for crack initiation at 1200 ft-lb. The problem thus was reduced to selecting the critical combination of stress and temperature that would provide complete fracture. The sequence of adjusting the stress and temperature can be followed in Table 5.

After the complete fracture in Test 2 at an average net stress of 16,000 psi and a temperature of 0°F, it was decided to alter only the stress on the next test. Test 3, at a stress of 14,000 psi, resulted in a 4 1/2-in. submerged crack. This tended to bracket the stress level for initiation and propagation at 0°F.

Test 4 was made to see if a crack would propagate at a higher temperature (20 F), but at the same stress as used in Test 2; the result was a 1-in.

submerged crack. Another test on the same insert, but on the opposite notch and at a higher stress, resulted in a 2-in. submerged crack. It appeared that complete fracture at 20 F would require a higher stress or perhaps higher impact energy for fracture initiation.

Thus it was concluded that a brittle fracture could be propagated consistently across the plate at an average stress of about 18,000 psi on the net section, at a temperature of about 0°F, and with an external impact energy of 1200 ft-lb for fracture initiation.

(d) Second Group (Tests 5--8)

The four specimens of this second group were instrumented with strain gages and speed detectors. Since only four channels of instrumentation were available for the first three specimens, two channels were used for strain and two channels were used for detectors. One additional channel became available for Test 8, and this provided three channels for strain measurements.

Dynamic strains were recorded for two vertically oriented strain gages mounted at the mid-width of the plate, 1 1/2 and 6 in. above the notch line. The reason for mounting one dynamic strain gage above the other at the mid-width of the plate was to investigate the change in strain pattern with increasing distance from the fracture path. In Test 8, the additional channel of instrumentation was used for a vertically oriented strain gage, located 18 in. from the striking edge and 1 1/2 in. above the notch line.

Each specimen also had a number of strain gages which were used to monitor the static strain values at various locations on the plate. In general, after Test 5, those gages that were used for dynamic strain readings had two companion gages, one mounted alongside the dynamic gage and the other mounted on the opposite surface of the specimen. As a part of the preloading operation at room temperature, all strain gages were read statically.

Each specimen of this group had five detectors mounted on each side. The detectors were mounted back-to-back, and all five detectors on one side were connected into one channel of the instrumentation. The speed detectors for this group of tests were concentrated toward the striking edge to check the variation in speed as the fracture progressed toward the center of the specimen. Generally, at least one detector was placed beside a dynamic strain gage to check the detector breaking time with the response of the strain gage.

Although there were five speed detectors on each side of the specimen mounted back-to-back, the detectors on each side were of different types. Since the consistency of even the same type of detector mounted back-to-back is questionable, the use of different types on opposite sides of the plate makes a cross-check of the advancing crack front unreliable. Moreover, it is impossible to state at what stage of crack development any one type of detector breaks. In some of the earlier work, it was noted that the passing of a submerged crack under a detector caused the detector to break. Such behavior tended to verify that the speed detectors are relatively sensitive to the passage of the crack, and that the speed values obtained from the detectors were fairly representative of the average crack speed. This belief is further borne out by the fact that in the third group of tests, Section 12(e), the speeds determined from the times of peaking of the strain traces as the crack approached and passed the gages approximately checked the speeds computed from the detectors.

The record shown in Fig. 33 for Test 5 is incomplete because of an incorrect choice of sweep time. Since the one-millisecond sweep time used for Test 1 resulted in a complete record, this same total sweep time was chosen for Test 5. However, for those specimens in which the fracture was initiated from a saw-cut notch in the region of a sheared edge (Test 5 and Test 7), there was a time delay in the initiation. A study of the data for these two tests indicates that the time required to propagate the first 1 3/4 in. beyond the first trigger is about 600 to

700 microseconds. This is to be compared with a corresponding value of about 150 microseconds for those specimens in which the crack started from a notch in interior plate material. The difference in fracture texture corresponding to the two types of initiation regions is discussed in Section 13.

The strain oscillations shown in Fig. 33 are not easily explained, unless they are the result of the initial propagation resistance mentioned in the preceding paragraph. However, this same type of initial strain behavior was not apparent in the record of Test 7 (Fig. 35), which experienced a delay of the same magnitude as Test 5.

In Figs. 34--36, it will be observed that the sharp, high strain peaks occur for those gages nearest the fracture path. However, the vertically oriented strain gages mounted 6 in. above the notch line show strain values that increase from time zero, as contrasted to the gages mounted closer to the crack that show essentially a steady or decreasing value of strain before the fracture approaches. The upper gages (those at the greater distance from the notch line) peak out at a smaller strain value but at an earlier time. This behavior was not entirely unexpected since the upper gage, by virtue of its position, can perceive the strain response sooner than the gage nearly in line with the fracture. The strain decay is most rapid for those gages near the fracture path, and a marked time-attenuation in gage response is noted for those gages 6 in. from the fracture path. The strains generally return to the absolute zero values after fracture. The variation in leveling-off strain may be caused in part by relaxation of residual strains, inelastic strain resulting from fracture, and stretching of the lead wires after fracture. The cyclic oscillations of the strains upon returning to absolute zero have been noted to check approximately with the natural frequency of the fractured half-specimen.

In Test 6--8, it will be observed that the detectors alongside the dynamic strain gages broke at about the same time, or slightly later than, the time at which the strain traces peaked.

(e) Third Group (Tests 9--11)

In the third group of tests, attention was concentrated on the strain pattern in the vicinity of the fracture. The instrumentation for the third group was much the same as that for the second group, except for the changes noted below. Beginning with Test 9, SR-4 Type A-7 strain gages were used. The speed detectors were single wire SR-4 Type A-9 strain gages. Only one set of detectors was distributed more or less uniformly across the width of one side of the specimen. This resulted in one channel of speed detectors and four channels of strain. One of the latter strain channels was connected to a strain gage, which was oriented horizontally and situated adjacent to a longitudinal gage at the mid-width of the plate. Photographic trouble resulted in the loss of all of the records for Test 9, with the exception of one vertically oriented strain gage. Also, the data beyond 0.59 milliseconds in Test 11 (Fig. 39) is questionable because of severe overlapping of the traces.

The stress-strain diagrams for the static preloading operation for Test 10 (before cooling) are presented in Fig. 40, and a similar diagram for the static readings during the cooling process is presented in Fig. 41. The position of the static strain gages is shown in Fig. 38. In general, the "before cooling" and "while cooling" values show reasonably close agreement. The difference in strains may be due in part to the small differences in the length of the lead wires, as noted in Section 10(b). Too, residual strains relieved by the loading process may have caused part of the discrepancies.

Since all of the vertically oriented dynamic strain gages are near the crack path, the records show relatively sharp strain peaks. In these particular tests, vertically oriented strain gages at an essentially constant distance from the crack path exhibit strain peaks that increase in magnitude as the distance between the gage position and the starting edge becomes greater. Generally, it is noted that as the distance between the strain gage and fracture path increases (for example,

compare Tests 10 and 11), the strain peak amplitude decreases, and the pulse time increases.

The horizontal strain gage mounted adjacent to the vertical strain gage at the mid-width of the plate (Fig. 38) shows a somewhat different behavior. As the crack approached the gage location, the horizontal strain reached a maximum, proceeded to a sudden minimum at the same time the vertical gage reached its maximum, continued to attain another maximum, and then exhibited cyclic oscillations.

In Tests 9 through 11, a detector was placed near each of the vertically oriented dynamic strain gages to check the detector's breaking time with the strain response. In general, the detectors broke after the peaking of the corresponding strain gage; this is logical because not only were the detectors on the far side of the strain gage, but theoretical considerations indicate that the strain gage should peak before the fracture reaches the gage location. Further evidence of this agreement is observed in Test 11, where the fracture path is farther away from the gage locations, and the time differences are greater.

In general, there does not appear to be any correlation between permanent set in the strain readings and distance of the gage from the fracture surface. For example, in this series of tests, the strain residuals ranged from 200 to -100 micro in./in.

A typical temperature-time relationship for Test 9 is shown in Fig. 42. The uniformity of the cooling is apparent from the temperature values recorded in this figure. The bottom portion of the curve has been expanded in Fig. 43 to show the slight temperature rise that was observed immediately after fracture. This rise in temperature can very likely be attributed to the energy released during fracture. The fact that the curve starts to drop again merely indicates that the cooling tanks against the specimen were still cooling immediately after the test. However, thermocouple No. 4, which was 6 in. from the fracture, also showed the same increase in temperature which suggests that the change may have been caused by some other factor.

A comparison of the various records in each of the groups reported here shows that, in general, consistent records are obtained for similar test conditions and instrumentation locations. This statement is particularly true for the strain traces, if the position of the gage with reference to the fracture is taken into consideration. For the first few tests, the crack speeds (Table 6) exhibited a tendency to increase with crack length; in the later tests, the crack speeds exhibited a tendency to reach a plateau after the first 6 to 12 in. of crack travel. The variations in crack speed may be due in part to differences in breaking properties of the detectors as noted in Sections 7 and 10(b), and as later studies indicate, a discontinuous surface fracture may account for some of the detector and strain gage anomalies that have been noted.[3]

13. Crack Path and Texture of Fracture Surfaces

Photographs of the plate fractures are presented in Figs. 44 through 52. In these figures, a string is stretched between the notches to help outline the path of the fracture with respect to the notch line. No preference for the crack to go above or below the notch-line was noted. The secondary cracks that often started from the notch cut at the far edge can be clearly observed in the photographs. Generally, the secondary crack joined the main fracture and resulted in a detached piece of plate material. It is believed that these secondary cracks may be the result of the localized high tension and other factors that occurred toward the end of the test. Various views of the detached pieces resulting from the secondary cracking are shown in Fig. 53.

The texture of the fractures may be noted in Figs. 44 through 52. The shear lip associated with all of these fractures was very small and almost imperceptible. In a careful examination of the fractures, it was noted that portions of the surface exhibited a coarse texture while other portions were fine. It was thought that there might be a correlation of this texture with the crack speed. However, after further study, it was found that, in general, no correlation of the

texture with the speed was evident. In Tests 2, 5 and 7, in which the fracture was initiated from a notch in the region of a sheared edge, the first several inches of the fracture surface had a coarse appearance. This may be seen in Figs. 45, 46 and 48. An enlarged view of this tough region is shown in Fig. 54, together with a view of the initiation region near a flame-cut edge; in the case where the edge was flame cut, none of the fractures exhibited the tough appearance. This interesting observation may perhaps be visualized more easily by referring to Fig. 20, which shows the layout of the specimens on the original plate. This behavior was not exhibited by Specimens Z1A8 and Z1A10 because their starting edges were located about 1/2 in. in from the sheared edge of the original plate (about 1/2 in. of the original sheared edge was burned off).

IV. SUMMARY

The object of this program is to study the propagation of brittle fractures in wide steel plates. This report describes the early development work on the program and the subsequent preliminary series of tests of 2-ft wide plate specimens.

Initially, two methods of fracture initiation were investigated, the powder detonator bolt, which involved the use of an explosive, and the notch-wedge-impact method. Although attractive for several reasons, the detonator bolt method failed to initiate any fractures and thus was dropped from further consideration. As a result, the notch-wedge-impact method of fracture initiation has been used for all plate tests in this program to date. Other development work included specimen cooling, instrumentation, and details of specimen geometry.

When the development work had progressed to a satisfactory stage, a series of tests of 2-ft wide specimens was made. These tests involved the surface measurement of crack speed and strain pattern while the fracture was propagating. Their

results may be summarized as follows:

1. Crack speeds ranging from 1150 to 5900 fps were recorded.
2. Absolute peak elastic strains as high as 2500 micro in./in. (0.0025 in./in.) have been recorded in the vicinity of the fracture.
3. For vertically oriented dynamic strain gages, as the distance from the fracture to the gage increases, the magnitude of the peak strain decreases, and the pulse time increases.
4. No correlation of crack speed with texture was noted.
5. A sizable delay in the time necessary to start full propagation was noted for cracks initiated in the vicinity of a sheared edge.

A comparison of the records from each group of tests indicates that, within reason, consistent data were obtained at similar gage locations under comparable test conditions.

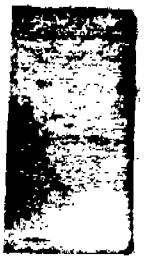

REFERENCES

1. Wilson, W. M., Hechtman, R. A., and Bruckner, W. H., Cleavage Fractures of Ship Plates (Engineering Experiment Station Bulletin Series No. 388), Urbana: University of Illinois, 1951.

2. Hall, W. J., Mosborg, R. J., and McDonald, V. J., "Brittle Fracture Propagation in Wide Steel Plates," The Welding Journal, 36:1, Research Supplement, 1s--8s, 1957.

3. Lazar, R., and Hall, W. J., Studies of Brittle Fracture Propagation in Six Foot Wide Structural Steel Plates (Civil Engineering Studies, Structural Research Series No. 136), Urbana: University of Illinois, 1957.

4. Robertson, T. S., "Propagation of Brittle Fracture in Steel," Journal of the Iron and Steel Institute, vol. 175, pp. 361--374, 1953.

5. Feely, F. J., Jr., Hrtko, D., Kleppe, S. R., and Northup, M. S., "Report on Brittle Fracture Studies," The Welding Journal, 33:2, Research Supplement, 99s--111s, 1954.

6. Feely, F. J., Jr., Northup, M. S., Kleppe, S. R., and Gensamer, M., "Studies on the Brittle Failure of Tankage Steel Plates," The Welding Journal, 34:12, Research Supplement, 596s--607s, 1955.

7. Williams, M. L., "Analysis of Brittle Behavior in Ship Plates," ASTM Special Technical Publication No. 158, pp. 11--44, 1953.

8. Puzak, P. P., Schuster, M. E., and Pellini, W. S., "Crack-Starter Tests of Ship Fractures and Project Steels," The Welding Journal, 33:10, Research Supplement, 481s--495s, 1954.

9. Mylonas,C., Drucker, D. C., and Isberg, L., "Brittle Fracture Initiation Tests," The Welding Journal, 36:1, Research Supplement, 9s--17s, 1957.

10. Boyd, G. M., "The Propagation of Fractures in Mild-Steel Plates," Engineering, pp. 65--69, January 16, 1953.

11. Wells, A. A., The Brittle Fracture Strength of Welded Steel Plates (Paper No. 6), The Institution of Naval Architects, presented at March 22, 1956, meeting.

12. Wells, A. A., "The Mechanics of Notch Brittle Fracture," Welding Research, 7:2, 34r--56r, 1953.

13. Roberts, D. K., and Wells, A. A., "The Velocity of Brittle Fracture," Engineering, pp. 820-821, December 24, 1954.

14. Orowan, E., "Fundamentals of Fatigue and Fracture of Metals" (MIT Symposium), New York: John Wiley & Sons, Inc., pp 154-155, 1952.

15. Irwin, G. R., "Fracturing and Fracture Dynamics," Transactions of the American Society for Metals, vol. 40 A, p. 147, 1948.

16. Irwin, G. R., and Kies, J. A., "Critical Energy Rate Analysis of Fracture Strength," The Welding Journal, 33:4, Research Supplement, 193s--198s, 1954.

17. Fettahlioglu, O. A., A Preliminary Investigation of Brittle Fracture Propagation in Structural Steel (M. S. Thesis submitted to the Graduate College, University of Illinois), 1956.

TABLE 1 SUMMARY OF PRINCIPAL TESTS INVOLVING THE POWDER DETONATOR BOLT

Test No.	Machine Load (kips)	Average Stress on Net Section (ksi)	Temp. (F)	Purpose of Test	Results
All of the following nine tests were conducted on E steel specimens from plates 16-1 or 17-A. The dimensions of the following three specimens were 3/4- x 2 1/2- x 24-in. (see Figs. 1 and 5). Stress raisers for the first test consisted of a 5/8 in. drilled hole with two 1/16 in. long jeweler's saw-cuts normal to the specimen axis (see Fig. 4).					
1-DB	44.0	33.5	12	To determine the effect of the explosive load under the stated test conditions.	Highly developed slip line pattern in vicinity of hole but no indication of fracture.
Stress raisers for the following two tests consist of a 5/8-in. diameter punched hole (see Fig. 4).					
2-DB	42.0	30.0	5	Same as test 1-DB	No evidence of slip lines, enlargement of hole, or fracture. Unburned powder showed that pressure reached ceiling value.
3-DB	50.5	35.8	20	Same as test 1-DB, except at higher stress.	No evidence of slip lines or fracture. Diameter of hole enlarged 0.005 in. in direction of specimen axis.

In tests 4 through 8, the specimens are 12 in. wide (see Fig. 6). Stress raisers for the following group of tests are one 5/8-in. drilled hole with jeweler's saw-cuts and one 5/8-in. diameter punched hole. In test 4-DB, the insert plate was 12 in. long. The succeeding three tests (5-DB, 6-DB and 7-DB) were all made on the same insert specimen (9 in. in length).

TABLE I (Continued)

Test No.	Machine Load (kips)	Average Stress on Net Section (ksi)	Temp (F)	Purpose of Test	Results
4-DB	242.0	30.0	10	To attempt initiation of a brittle fracture with the detonator bolt in a 12-in. wide plate.	No fracture. Heavy yield patterns. Average diameter enlargement of 0.007 in.for punched hole and 0.015 in. for drilled hole.
5-DB	242.0	30.0	10	To check the yield pattern from static axial tension only in a 12-in. wide specimen. Detonator Bolt was not fired.	Very small yield pattern caused by axial tension alone.
In the next two tests the bolt was used with a hydraulic pump as a static pressurizing device.					
6-DB	242.0	30.0	60	To determine the effect of hydraulic pressurizing of a drilled stress raiser.	Bolt seals broke at a hydraulic pressure of 33,000 psi.
7-DB	300.0	37.2	60	To attempt to initiate a brittle fracture by hydraulic pressurizing at a higher stress than used in Test 6-DB.	No evidence of fracture. Bolt seals broke at a hydraulic pressure of 22,000 psi.
8-DB	344.9 (at failure)	42.7 (at failure)	-2	To determine nominal breaking stress of a specimen subjected to only static load. Detonator bolt was not used.	Complete brittle fracture initiated in punched hole after considerable yielding (see Fig. 8).

TABLE 1 (Continued)

Test No.	Machine Load (kips)	Average Stress on Net Section (ksi)	Temp. (F)	Purpose of Test	Results
The following specimen was 9 in. x 3/4 in. at the net section (see Fig. 7). Stress raiser is one punched semi-circular hole (5/8 in. diameter) on edge of specimen. Specimen was eccentrically loaded. Detonator bolt was not used.					
9-DB	292.7 (at failure)	44.9	-5 at stress raiser, -10 at far side	Eccentric tension test to investigate possible stress correlation with previous test.	Complete brittle fracture after considerable yielding (see Fig. 9).

TABLE 2 CHECK ANALYSES OF STEEL PLATE MATERIAL

Material (Plate No.) Heat No.	Chemical Composition in Per Cent								
	C	Mn	P	S	Si	Cu	Cr	Ni	Al
Steel E (16-1) 20279	0.20	0.33	0.019	0.031	0.04	0.17	0.11	0.62	0.003
Steel E (17-A) 20279	0.21	0.34	0.019	0.030	0.01	0.18	0.12	0.19	0.003
Rimmed Steel (Z1A) 16445	0.18	0.42	0.013	0.031	0.02	0.23	0.07	0.14	0.003

TABLE 3 TENSILE TEST DATA OF STEEL PLATE MATERIAL

(Standard ASTM 0.505-in. dia. specimens)

Material (Plate No.) Heat No.		Lower Yield Strength (ksi)	Maximum Strength (ksi)	Per Cent Reduction of Area	Per Cent Elongation in 2-in.
Steel E (16-1) 20279	(L)	30.5	61.3	60.3	35.2
	(T)	29.6	60.7	56.3	35.2
Steel E (17-A) 20279	(L)	32.0	65.0	56.7	35.8
	(T)	31.8	64.4	53.7	31.0
Rimmed Steel (Z1A) 16445	(L)	34.7	68.1	57.6	36.5
	(T)	35.2	68.7	51.6	31.2

(L) Average of two specimens taken parallel to the direction of rolling.
(T) Average of two specimens taken transverse to the direction of rolling.

TABLE 4 SUMMARY OF DEVELOPMENT TESTS OF TWO FOOT WIDE PLAIN PLATE SPECIMENS

Specimen Insert No.	Steel Material (Plate No.)	Insert Test No.	Initial Load (kips)	Average Stress on Net Section (ksi)	Type of Notch and Wedge*	Theor. Impact Energy (ft-lb)	Average Temp. (F)	Remarks
A-1	A-285 Firebox Grade C	1	135	8.6	A	675	8	No fracture
		2	180	11.4	A	1100	2	No fracture
		3	225	14.2	A	1320	2	No fracture
		4	284	18.0	A	2200	-10	Complete fracture
E-1	E Steel (16-1)	1	212	14.0	A-1	410	-10	No fracture
		2	250	16.5	A-1	410	2	No fracture
E-2	E Steel (16-1)	1	223	14.0	B	700	- 9	No fracture
		2	241	15.0	C	700	26	Short submerged cracks to special slots
		3	241	15.0	C-1	700	28	2 3/4-in. submerged crack
E-3	E Steel (16-1)	1	247.5	15.0	C-2	700	26	2 1/2-in. submerged crack
		2	255	17.0	C-2	700	28	7/8-in. submerged crack
		3	252	18.0	C-2	700	26	Re-strike of the same notch as Test 2; slight extension of the submerged crack
E-3 (Bottom half of original Specimen E-3)		4	247.5	15.0	C-2	700	6	No fracture
		5	247.5	15.0	C-2	1200	0	Complete fracture

*A description of the types of wedges and notches used can be found by referring to their key letter at the end of this table.

TABLE 4 (Continued)

Specimen Insert No.	Steel Material (Plate No.)	Insert Test No.	Initial Load (kips)	Average Stress on Net Section (ksi)	Type of Notch and Wedge	Theor. Impact Energy (ft-lb)	Average Temp. (F)	Remarks
E-11	E Steel (17-A)	1	165	10.0	C-2	500	72	Striking test; no fracture
		2	165	10.0	C-2	1200	72	Striking test; no fracture
		3	272	16.5	C-2	1200	30	Complete fracture
E-10	E Steel (17-A)	1	273	16.5	C-2	1200	39	2-in. submerged crack
		2	285	19.0	C-2	1200	36	3-in. submerged crack

Type of Notch and Wedge

A 3-deg tapered wedge. Details are shown in Fig. 13(a).

A-1 Similar to wedge type A, except the notch is in the edge of the specimen.

B Circular tapered wedge, 20-deg included angle. Details are shown in Fig. 13(b).

C 7/8-in. four blade hacksaw cut followed by 1/4-in. single hacksaw cut and 1/8-in. jeweler's saw-cut. Some special diagonal saw cuts were made above and below the slot to concentrate the wedging action, but this was not successful.

C-1 Same as C without the special saw cuts.

C-2 7/8-in. four-blade hacksaw cut followed by 1/16-in. single hacksaw cut and 1/16-in. jeweler's sawcut. The outside edge of the notch was ground to fit the tapered wedge. This notch was used in all subsequent tests noted in this report. Details are shown in Fig. 13(c).

TABLE 5 PRELIMINARY TEST SERIES - TWO FOOT WIDE SPECIMENS

Test No.	Specimen No. and Date of Test	Initial Load (kips)	Average Stress on Net Section (ksi)	Average Temp. (F)	Remarks
These tests were conducted on 2-ft wide specimens of rimmed steel in the 600,000-lb Riehle testing machine. The brittle fracture was initiated by the notch-wedge-impact method with an impact of about 1200 ft-lb. The test piece was an insert (3/4- x 18- x 24 in.) welded to the 3/4-in. thick pull plates to provide a test piece 2-ft wide x 6-ft long in plan dimension (exclusive of the pull heads). The notch was 1-in. long and consisted of a slot four hacksaw blades wide (~0.141 in.) for the first 7/8 in., one blade wide (~0.034 in.) for the next 1/16 in., and ended with a jeweler's saw-cut (~0.012 in.) 1/16 in. long.					
1	E-18 8-11-55	412.5	25.0	13	Complete fracture. Excellent record.
2	Z1A1 9-9-55	264.0	16.0	-1	Complete fracture. No instrumentation.
3	Z1A2 9-13-55	231.0	14.0	0	Final load--227.9 kips. Submerged crack 4.5 in. long. No instrumentation.
4	Z1A3 9-22-55 (two tests)	264.0	16.0	20	Final load--262.0 kips. Submerged crack 1 in. long. No instrumentation.
		268.0	17.0	20	Final load--266.0 kips. Submerged crack 2 in. long. No instrumentation.
5	Z1A4 10-7-55	297.0	18.0	1	Complete fracture. Record good for the part that exists.
6	Z1A5 10-13-55	297.0	18.0	0	Complete fracture. Record poor. Instrumentation same as Z1A4.

TABLE 5 (Continued)

Test No.	Specimen No. and Date of Test	Initial Load (kips)	Average Stress on Net Section (ksi)	Average Temp. (F)	Remarks
7	Z1A6 10-20-55	297.0	18.0	1	Complete fracture. Good record. Instrumentation same as Z1A4.
8	Z1A7 10-31-55	297.0	18.0	-3	Complete fracture. Retriggered record of fair quality. Essentially another duplicate of Z1A4.
9	Z1A8 11-10-55	297.0	18.0	-2	Complete fracture. Record lost with the exception of one strain channel.
10	Z1A9 11-17-55	297.0	18.0	-5	Complete fracture. Good record. Instrumentation same as Z1A8.
11	Z1A10 11-23-55	297.0	18.0	-5	Complete fracture. Retriggered record of fair quality. Essentially another duplicate of Z1A8.

TABLE 6 CRACK SPEEDS FROM DETECTOR RECORDS

All distances are measured along the crack path.
Speeds are rounded off to nearest 50 fps.

etector Number	Measured Distance Between Detectors (in.)	Time Interval (μ - sec.)	Speed (fps)
Test 1 (E-18) East side (Silver-printed Detectors)			
A			
	2.0	40	4150
B			
	2.16	50	3600
C			
	3.90	85	3800
D			
	7.96	165	4000
E			
Test 1 (E-18) West side (Bismuth Wire Detectors)			
F			
	1.90	68	2350
G			
	3.96	70	4700
H			
	4.06	95	3550
I			
	4.01	80	4200
J			
Test 6 (Z1A5) East side (Silver-printed Detectors)			
A			
	2.48	73.0	2850
B			
	3.57	97.3	3050
C			
	3.46	103.2	2800
D			
	4.97	121.7	3400
E			

Detector Number	Measured Distance Between Detectors (in.)	Time Interval (μ - sec.)	Speed (fps)
Test 6 (Z1A5) West side (Bismuth Wire Detectors)			
F			
	2.36	33.2	5900
G			
	3.62	85.4	3550
H			
	3.53	94.1	3150
I			
	4.95	108.3	3800
J			
Test 7 (Z1A6) East side (Silver-printed Detectors)			
A			
	2.45	160	1300
B			
	3.58	140	2150
C			
	3.50	110	2650
D			
	4.95	70	5900
E			
Test 7 (Z1A6) West side (Bismuth Wire Detectors)			
F			
	2.43	180	1150
G			
	3.55	110	2700
H			
	3.54	110	2700
I			
	4.93	90	4550
J			

TABLE 6 (Continued)

Detector Number	Measured Distance Between Detectors (in.)	Time Interval (μ - sec.)	Speed (fps)
Test 8 (Z1A7) East side (Silver-printed Detectors)			
A			
	2.47	135.0	1550
B			
	3.53	103.2	2850
C			
	3.55	97.3	3050
D			
	4.93	139.7	2950
E			
Test 8 (Z1A7) West side (Bismuth Wire Detectors)			
F			
	2.48	97.5	2100
G			
	3.47	87.5	3300
H			
	3.65	107.5	2850
I			
	4.89	137.7	2950
J			

Detector Number	Measured Distance Between Detectors (in.)	Time Interval (μ - Sec.)	Speed (fps)
Test 10 (Z1A9) East side (A-9 Detectors)			
A			
	3.5	134.7	2150
B			
	4.5	111.9	3350
C			
	3.0	62.7	4000
D			
	4.5	112.7	3350
E			
Test 11 (Z1A10) East side (A-9 Detectors)			
A			
	3.5	127	2300
B			
	4.5	134	2800
C			
	3.0	91	2750
D			
	4.5	100	3750
E			

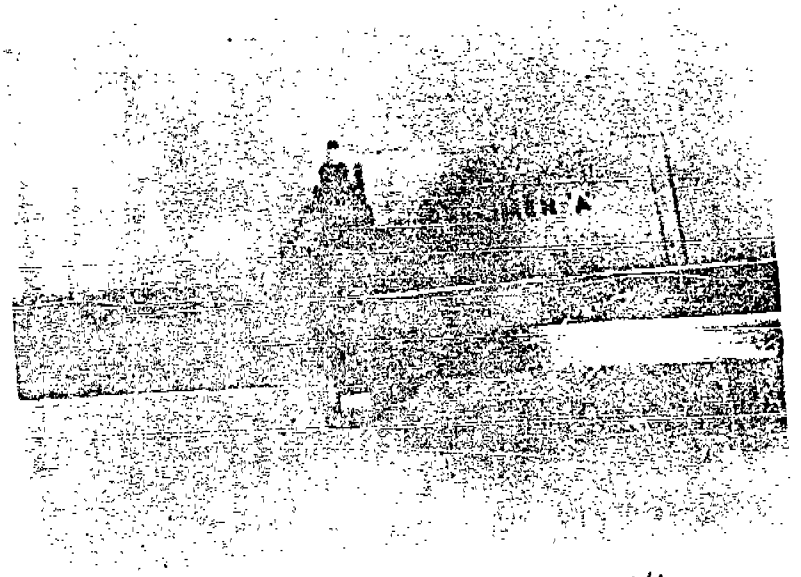

FIG. 1 FRACTURE INITIATION SPECIMEN, 3/4- x 2-1/2-in. PLATE, WITH DETONATOR BOLT

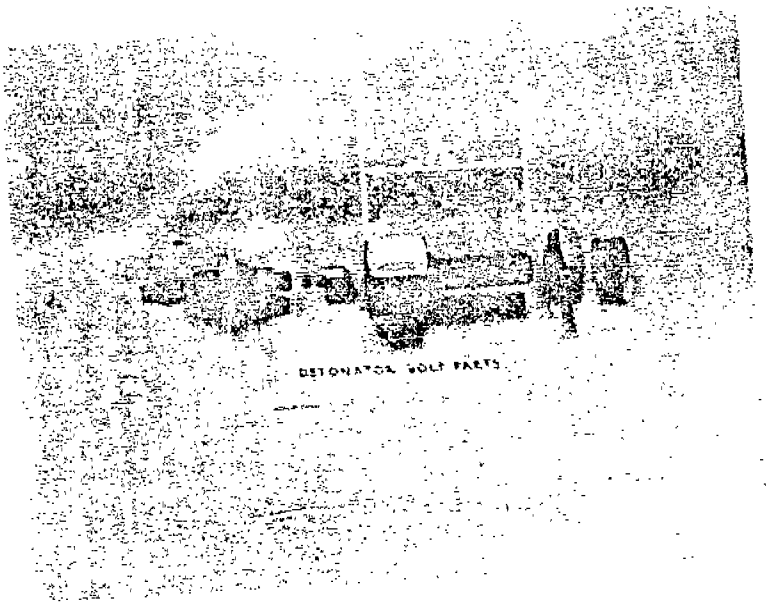

FIG. 2 DETONATOR BOLT PARTS, SHOWING SEALING RINGS IN POSITION

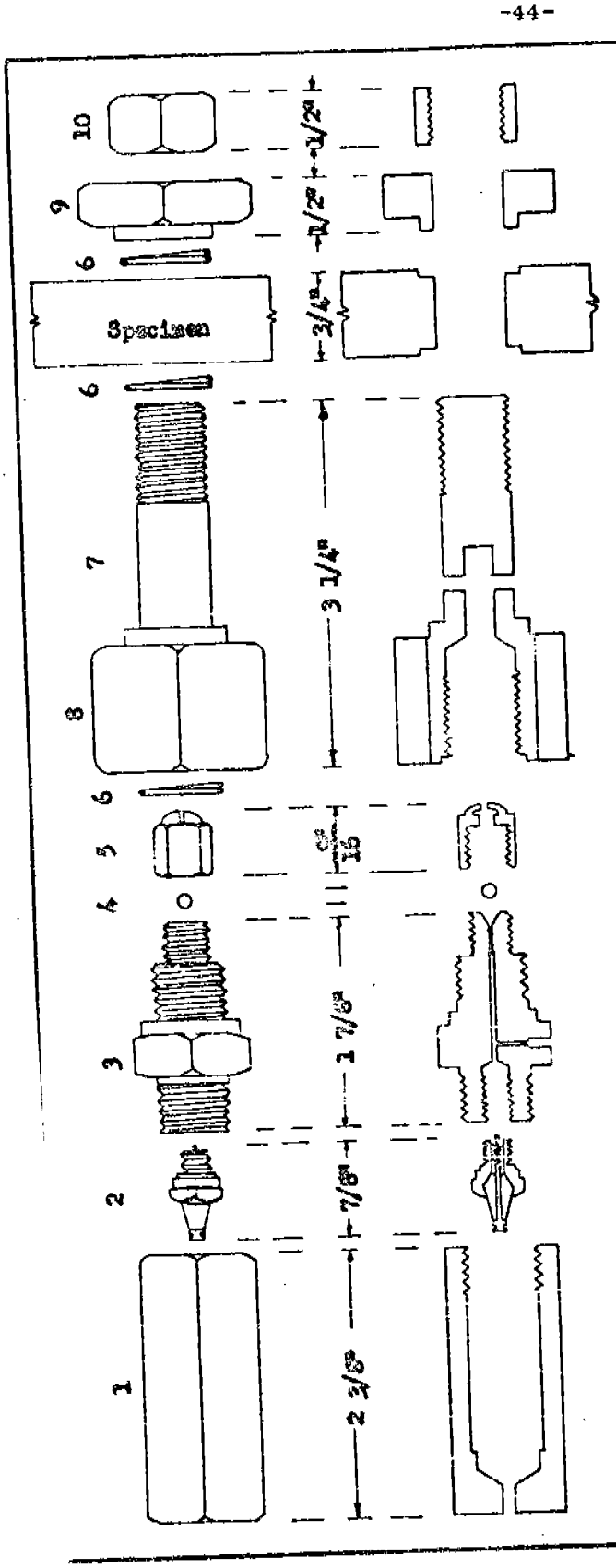

PART NO.	MATERIAL
1	1" Hexagonal Mild Steel
2	Gland-Sleeve Champion Type W2
3	1" Hexagonal Mild Steel, Cone Ended Valve Seating
4	5/32" Diameter Steel Ball
5	1/2" Hexagonal Mild Steel
6	3 - No. 0.052" Resin-cored Solder, Ring Seals
7	High Tensile Steel Machine Bolt
8	1 1/2" Hexagonal Mild Steel, Shrunk on Part No. 7
9	1 1/2" Hexagonal Mild Steel
10	5/8" Diameter Hexagonal Nut

FIG. 3 DETAILS OF POWDER DECOMPOSITION METER DEVICE

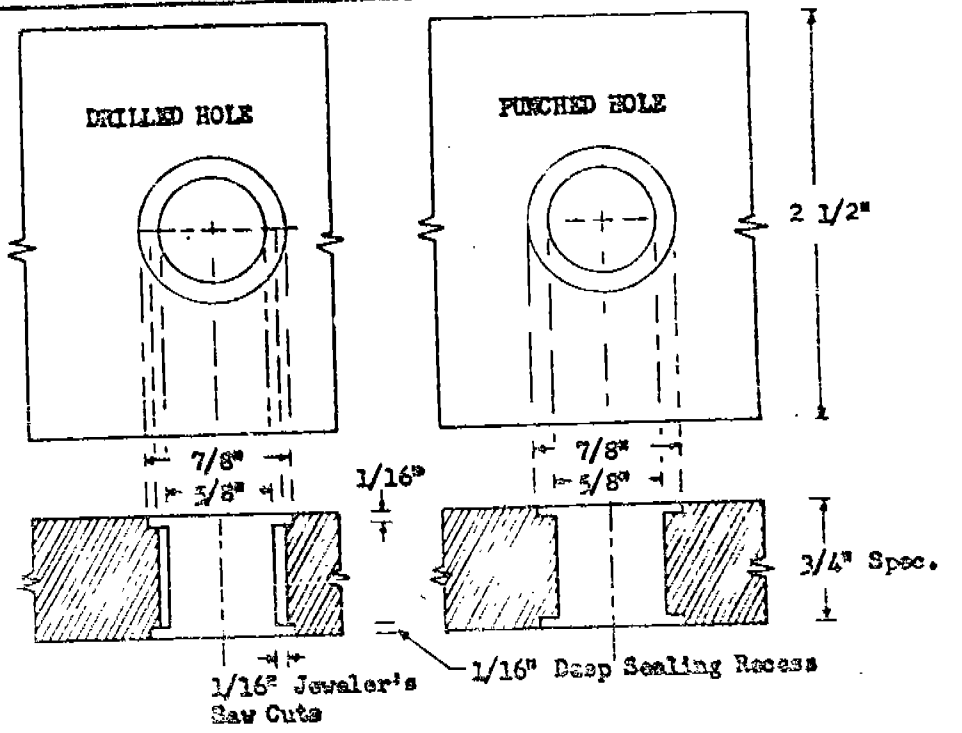

FIG. 4 DETAILS OF STRESS RAISERS FOR DETONATOR BOLT SPECIMEN

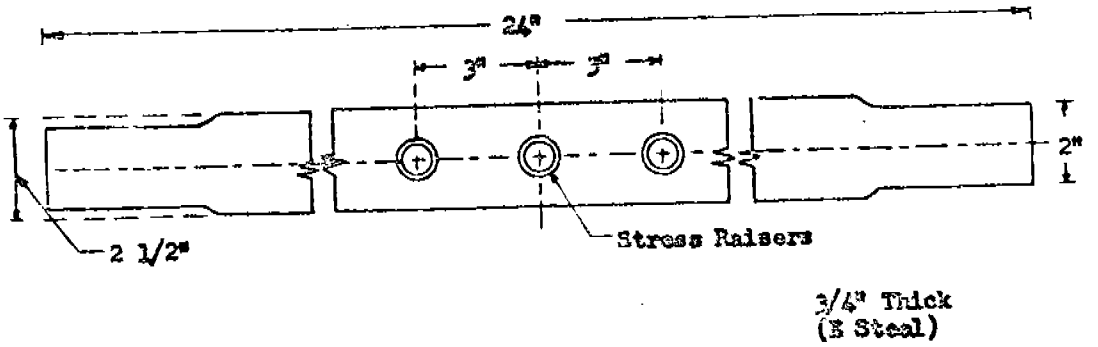

Note: Ends of Specimen Reduced to 2" Width to Fit Grips of Testing Machine

FIG. 5 DETAILS OF 3/4- x 2-1/2- x 24-in. SPECIMEN FOR DETONATOR BOLT

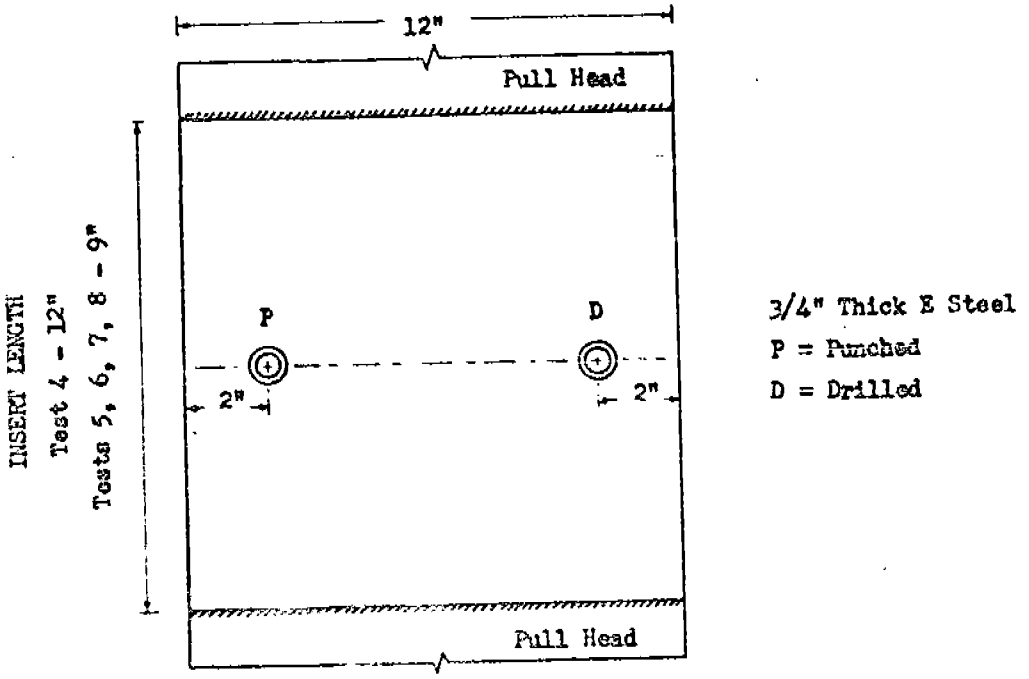

FIG. 6 DETAILS OF 3/4- x 12-in. SPECIMEN

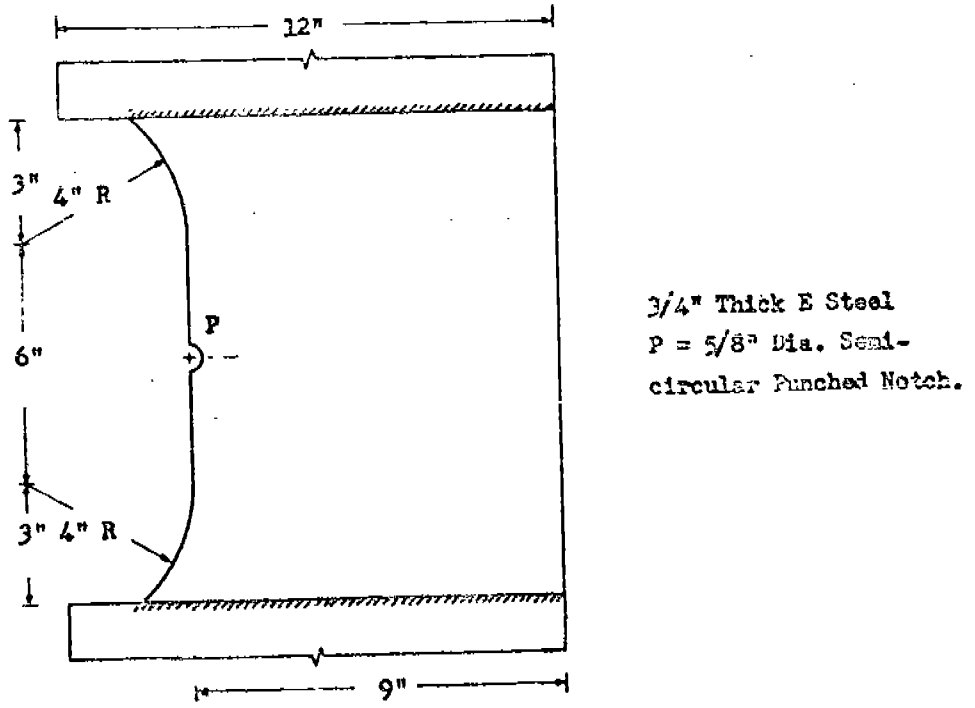

FIG. 7 DETAILS OF SPECIAL SPECIMEN FOR ECCENTRIC LOADING

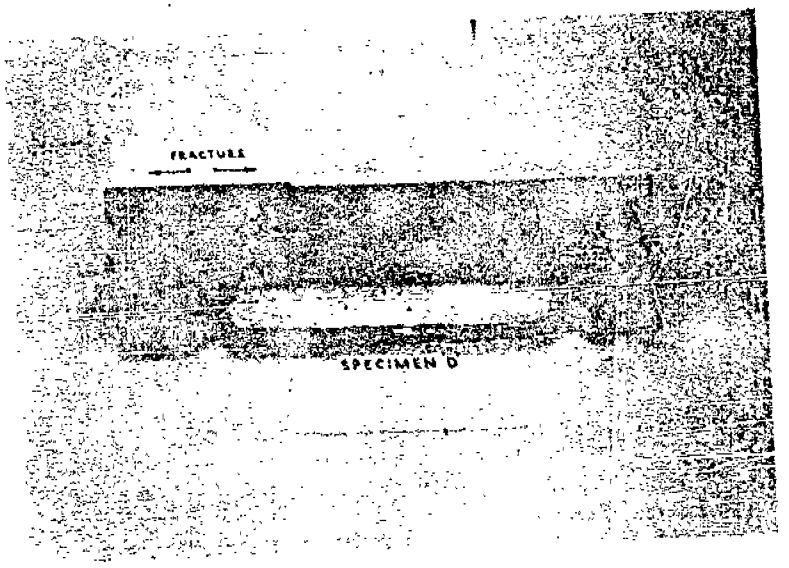

FIG. 8 FRACTURE INITIATION SPECIMEN, 3/4- x 12-in. PLATE AFTER STATIC TEST 8-DB — FRACTURE INITIATED FROM PUNCHED HOLE ON LEFT

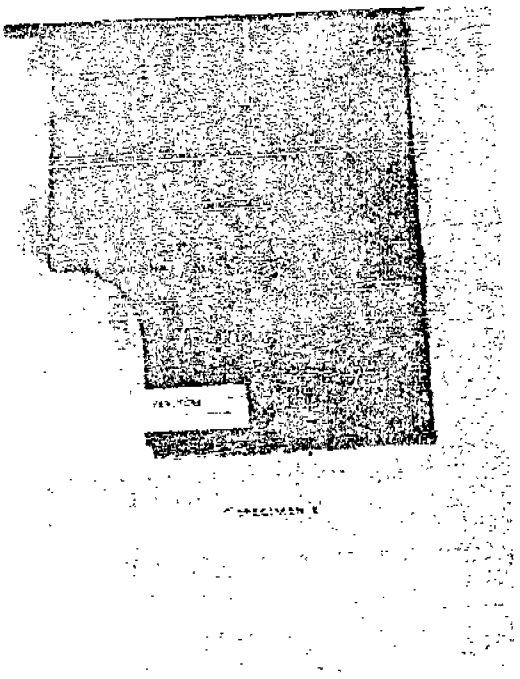

FIG. 9 ECCENTRIC TENSILE SPECIMEN AFTER STATIC TEST 9-DB — FRACTURE INITIATED FROM PUNCHED SEMICIRCULAR NOTCH

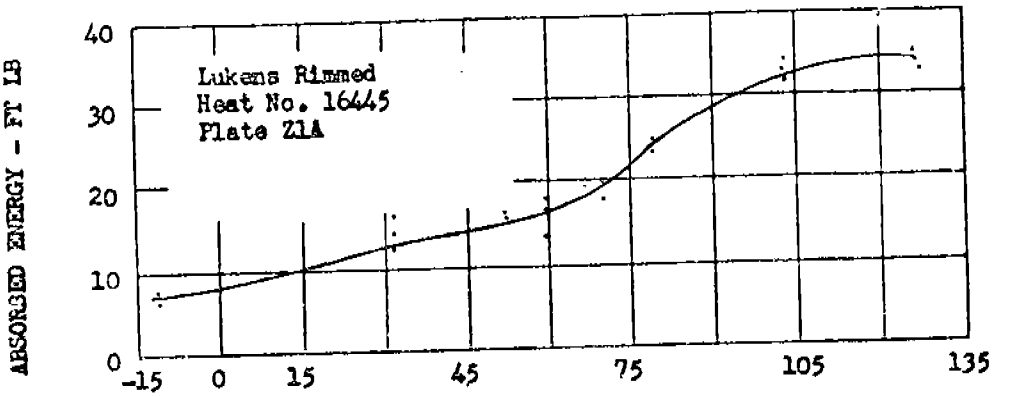

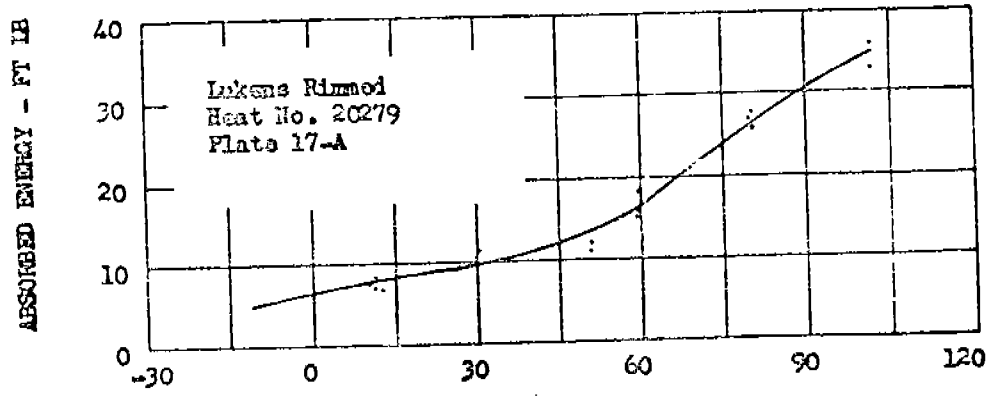

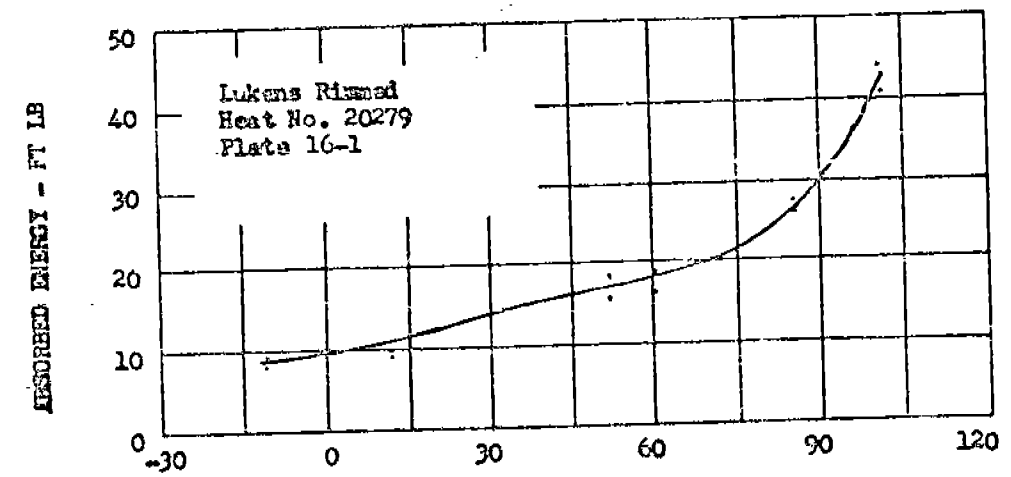

FIG. 10 CHARPY V-NOTCH IMPACT TEST RESULTS

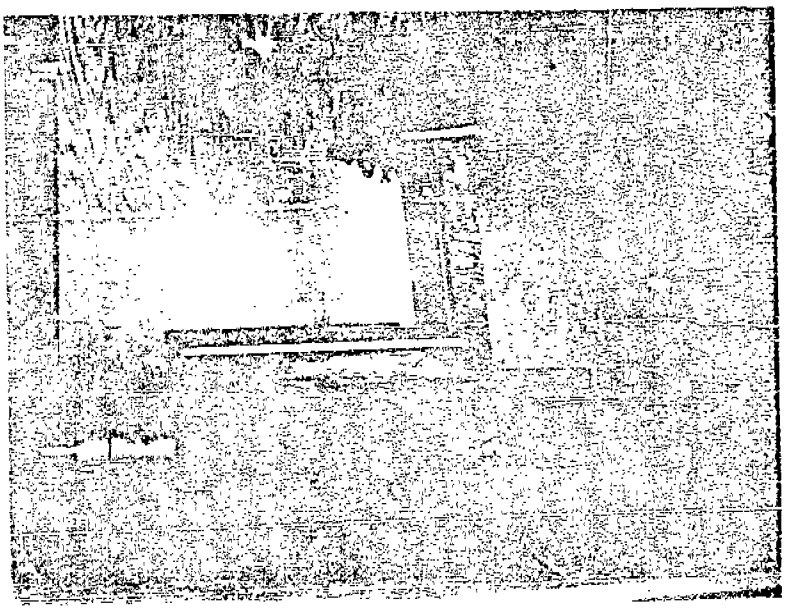

FIG. 11 GAS-OPERATED PISTON DEVICE — AFTER FIRING

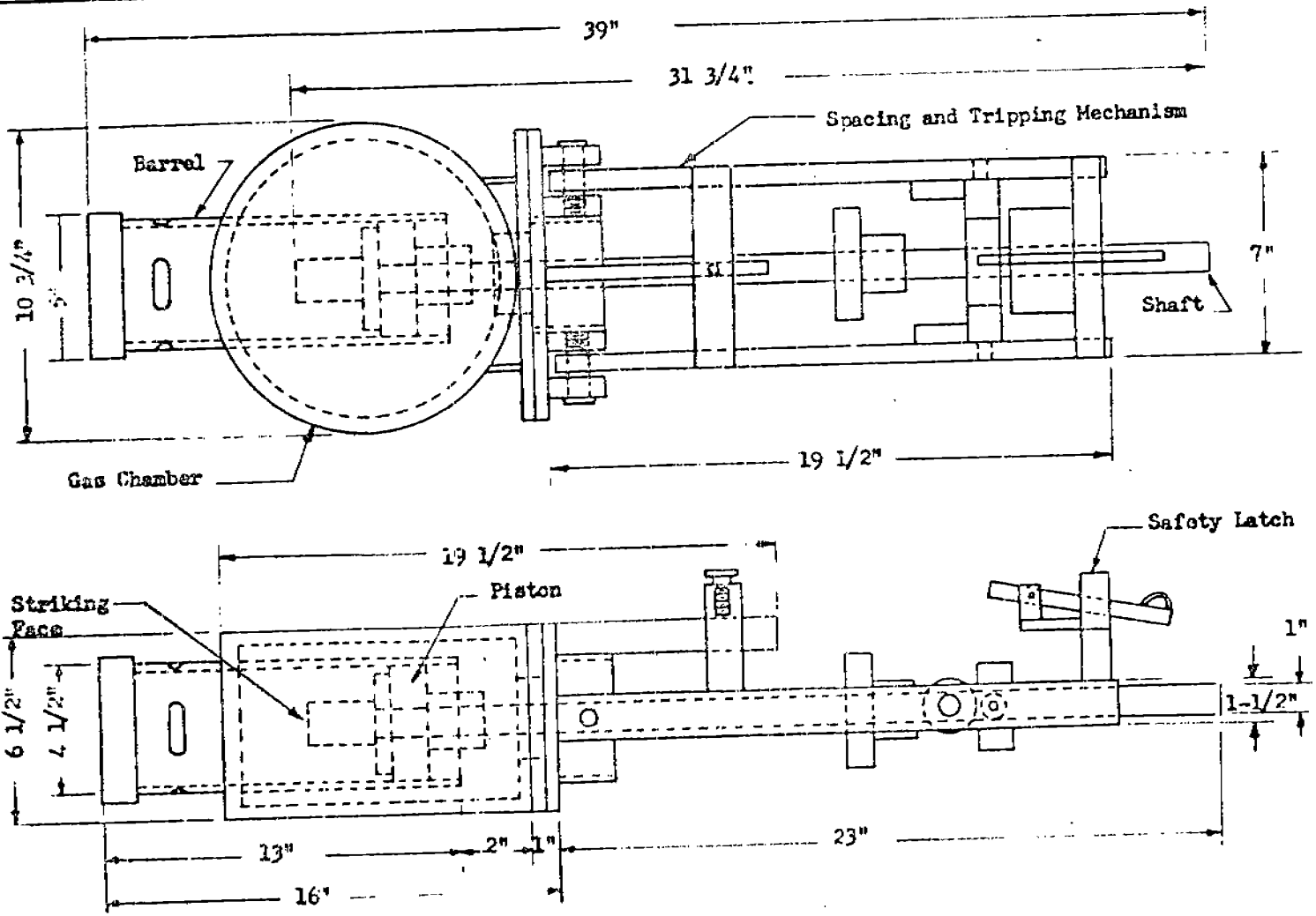

FIG. 12 GAS-OPERATED PISTON DEVICE

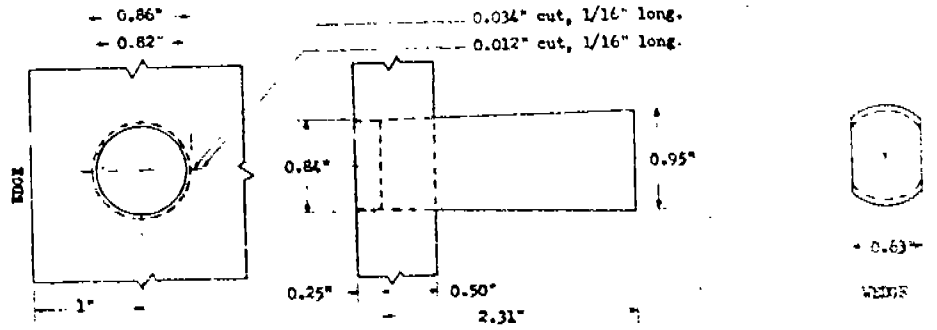

(a) Trial Method of Wedging (Broadside)

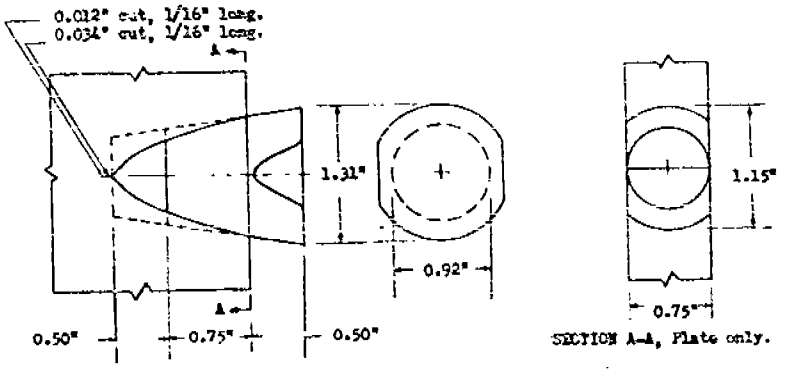

(b) Trial Method of Wedging (Edge-on)

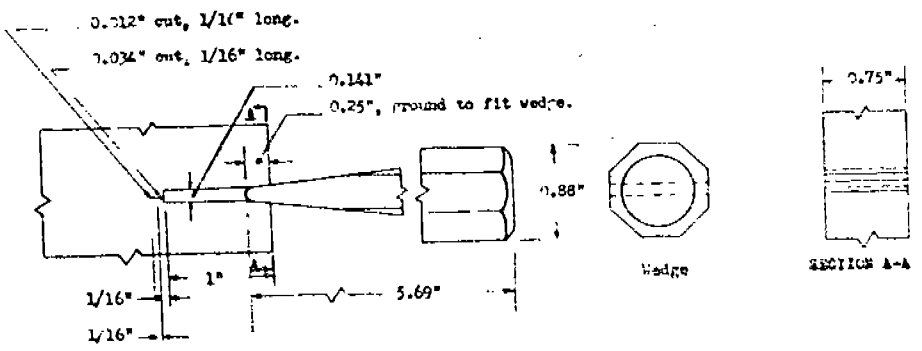

(c) Adopted Method of Wedging (Edge-on)

FIG. 13 WEDGE AND NOTCH DETAILS — USED FOR FRACTURE INITIATION

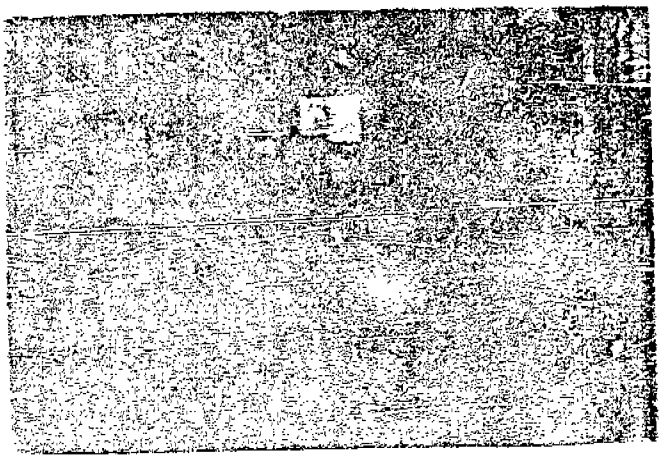

FIG. 14 SPECIMEN A-1 — AFTER TEST — BROADSIDE WEDGING

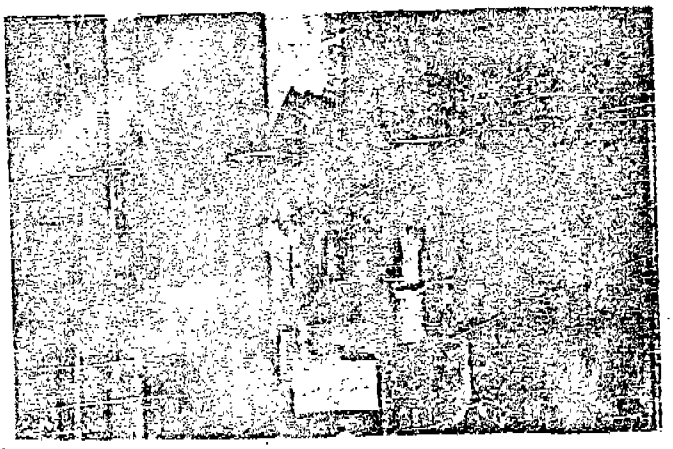

FIG. 15 SPECIMEN E-3 (BOTTOM HALF) — AFTER FRACTURE

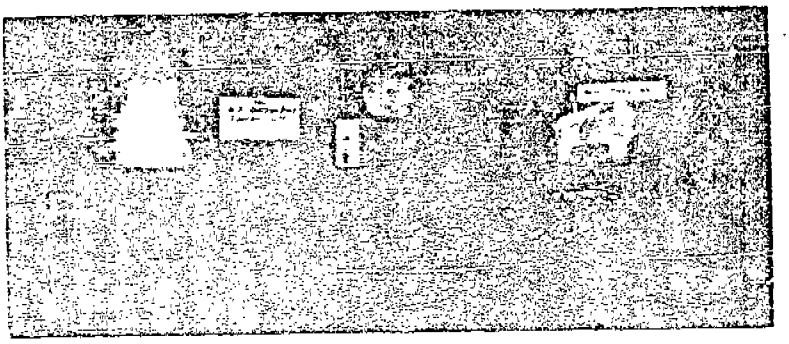

FIG. 16 SPECIMEN E-3 (BOTTOM HALF) — FRACTURE SURFACE

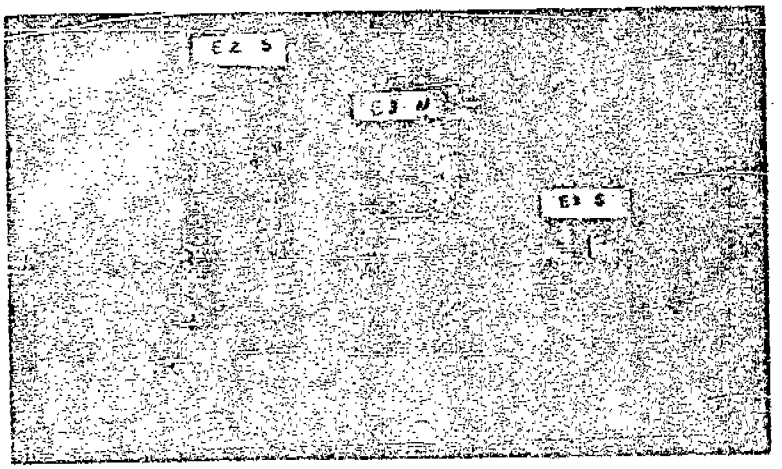

FIG. 17 FRACTURE SURFACE OF SUBMERGED CRACKS

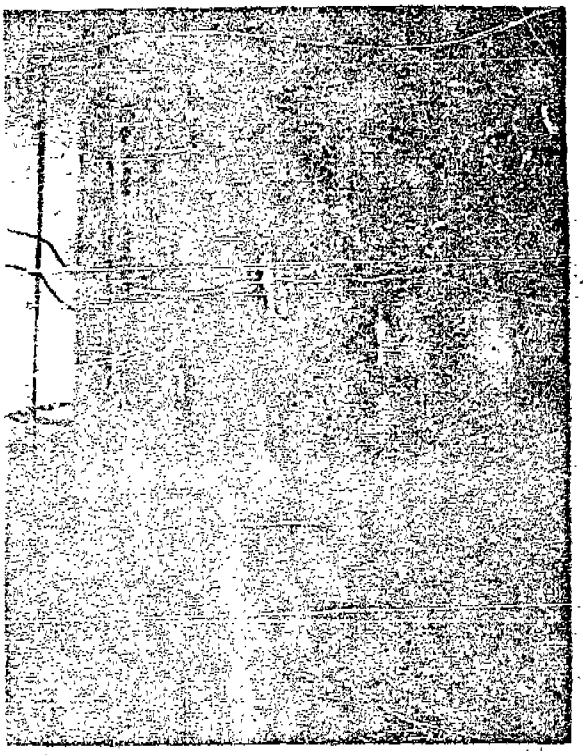

FIG. 18 TEST SETUP FOR EARLY DEVELOPMENT TEST

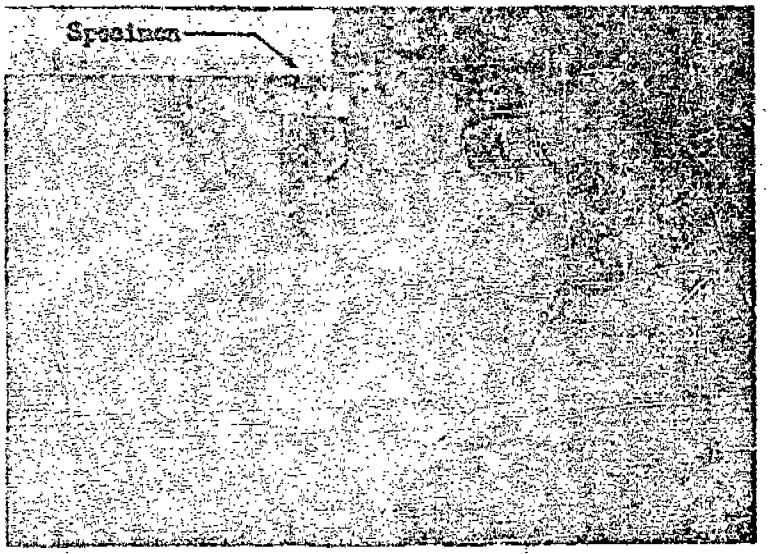

FIG. 19 DETECTOR CONSISTENCY TEST IN 20 KIP PULSE LOADING DEVICE

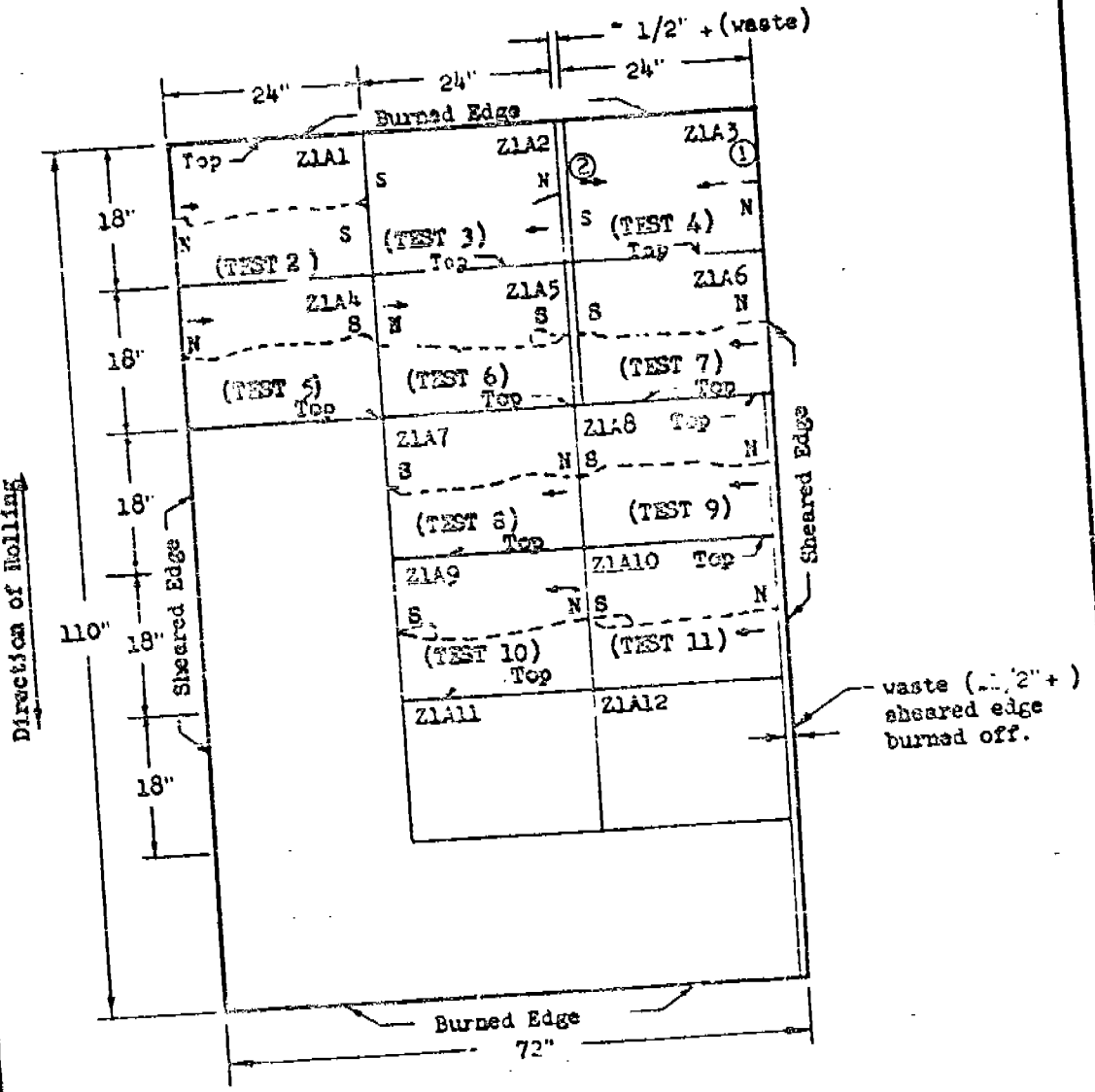

Notes: Lukens Rimmed Steel
Heat No. 16445
72" x 110" x 3/4" -- Plate 1A
All specimens struck on N Edge (Noted 'N")
Top - refers to orientation in 600,000-lb. testing machine.

FIG. 20 LAYOUT OF 2-FT WIDE Z1A SERIES SPECIMENS (TESTS 2 THROUGH 11)

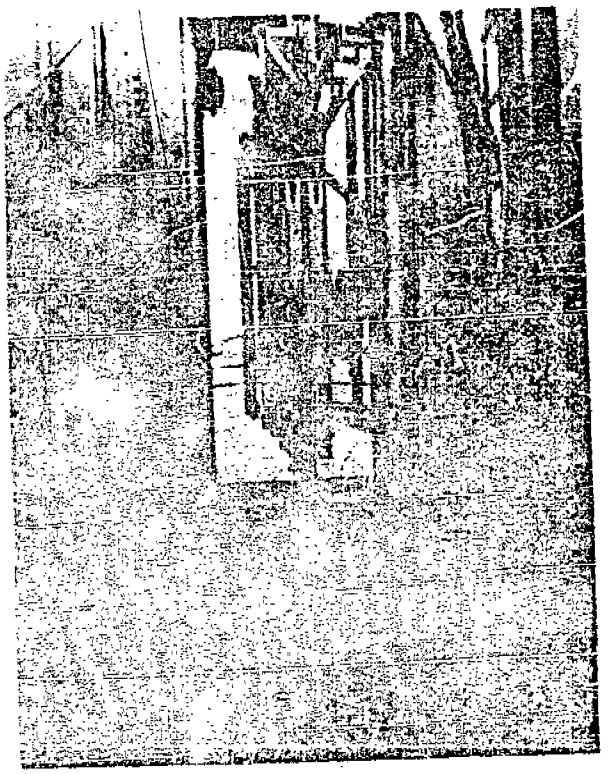

FIG. 21 TYPICAL TEST SETUP FOR Z1A SERIES — BEFORE FIRING

FIG. 22 COOLING TANK

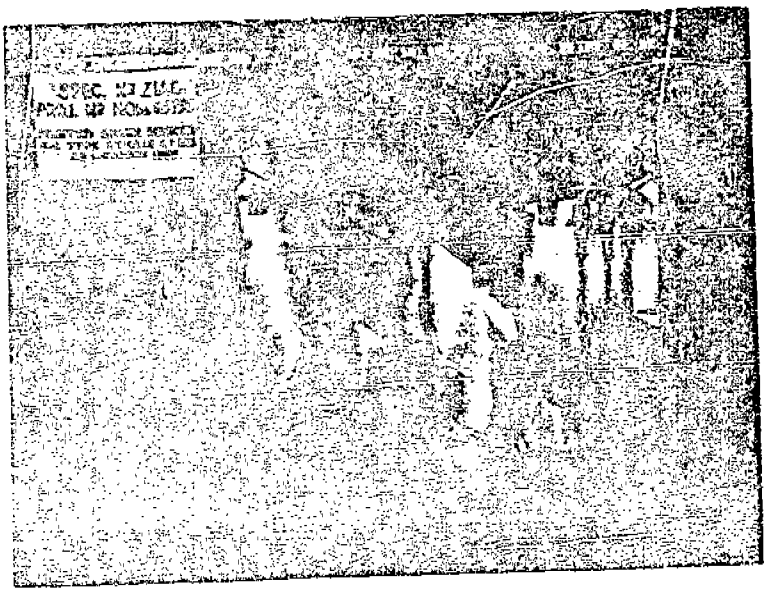

FIG. 23 EAST SIDE OF SPECIMEN Z1A6 (TEST 7) BEFORE TEST

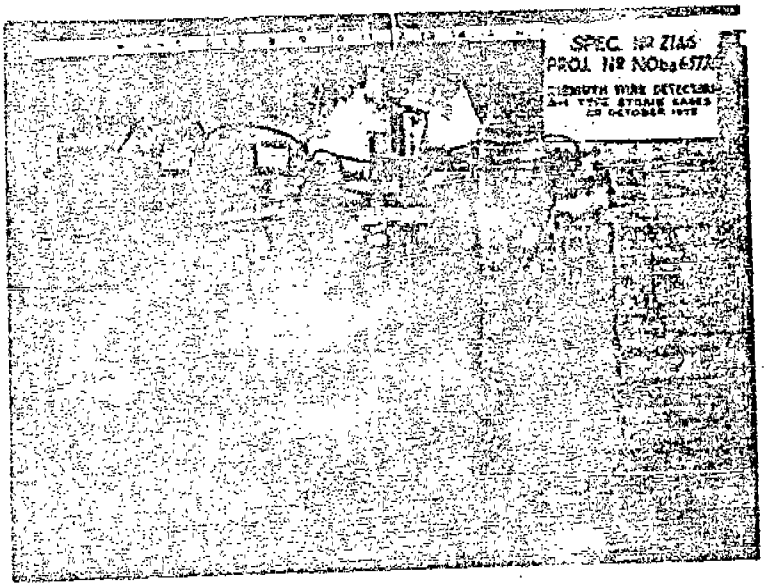

FIG. 24 WEST SIDE OF SPECIMEN Z1A6 (TEST 7) BEFORE TEST

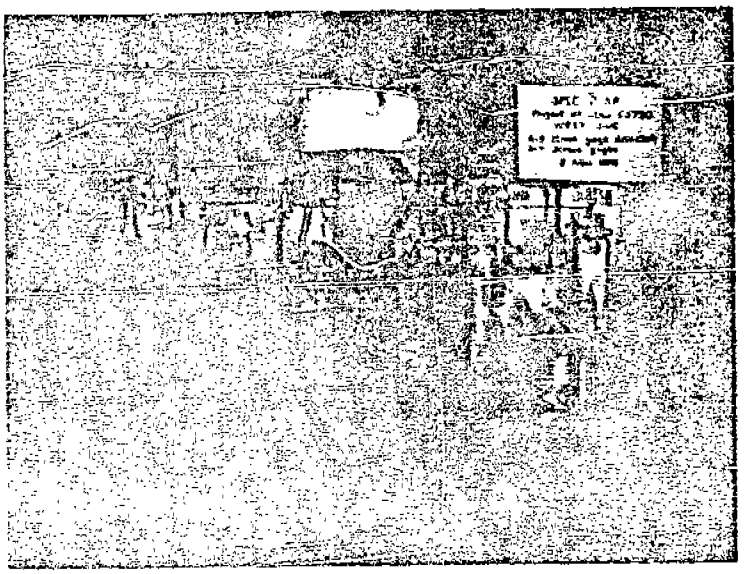

FIG. 25 WEST SIDE OF SPECIMEN Z1A8 (TEST 9) BEFORE TEST

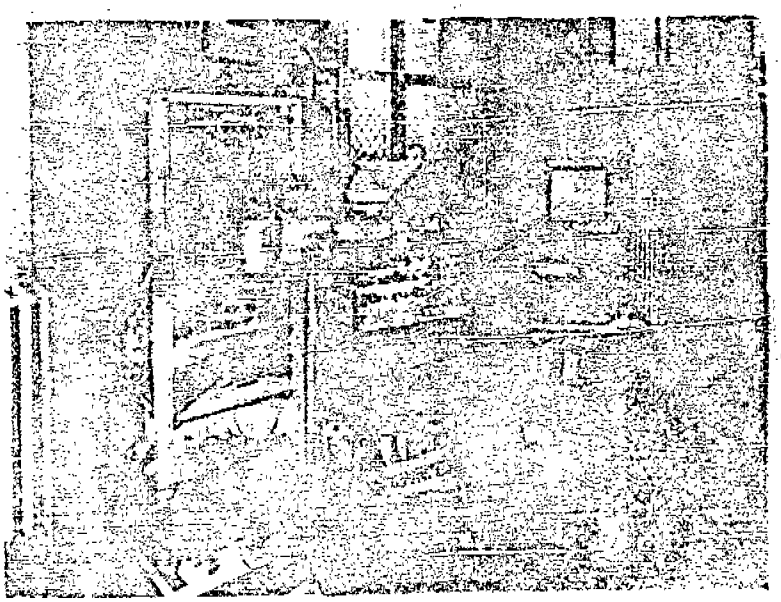

FIG. 26 RECORDING INSTRUMENTATION

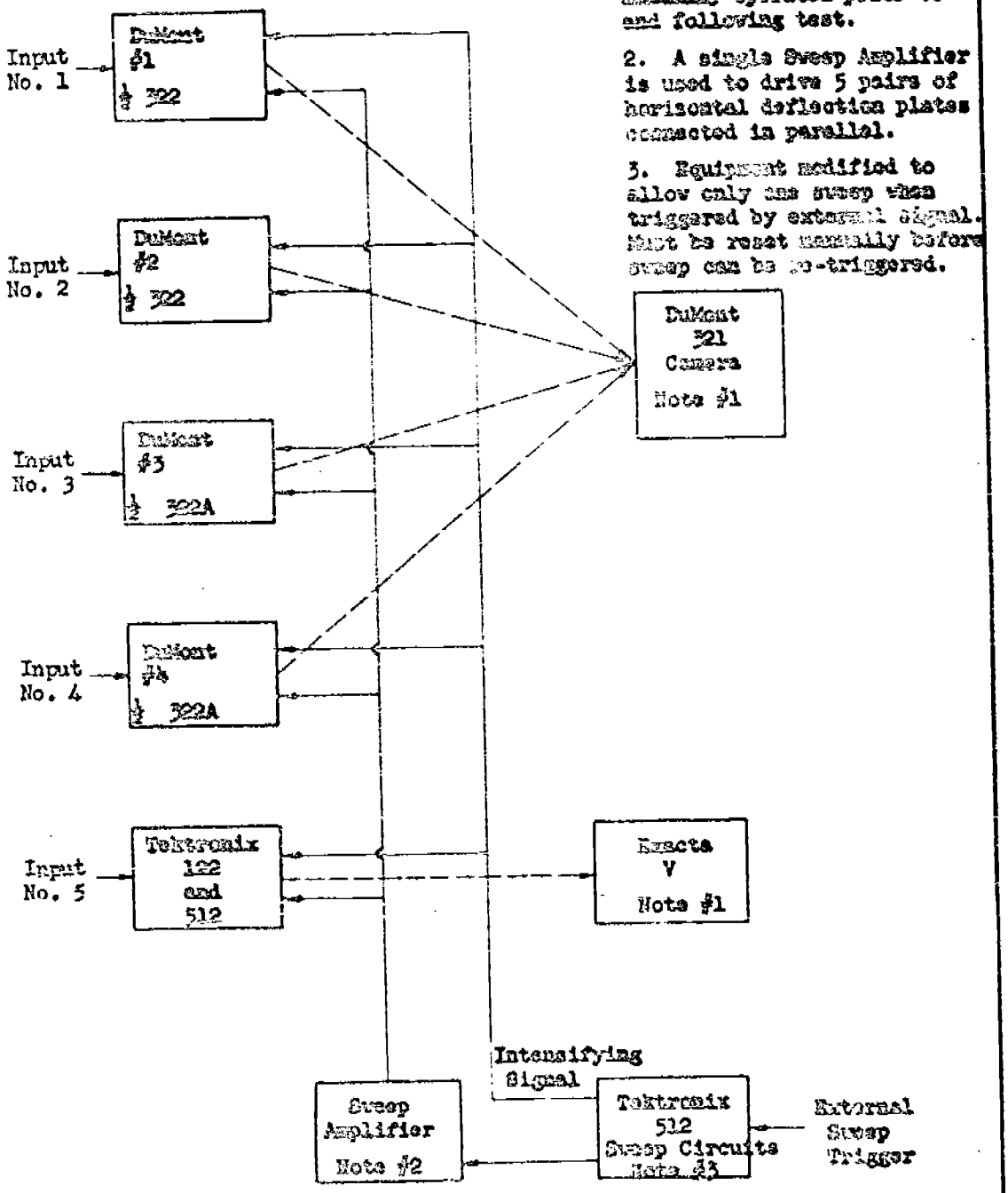

FIG. 27 BLOCK DIAGRAM OF RECORDING EQUIPMENT

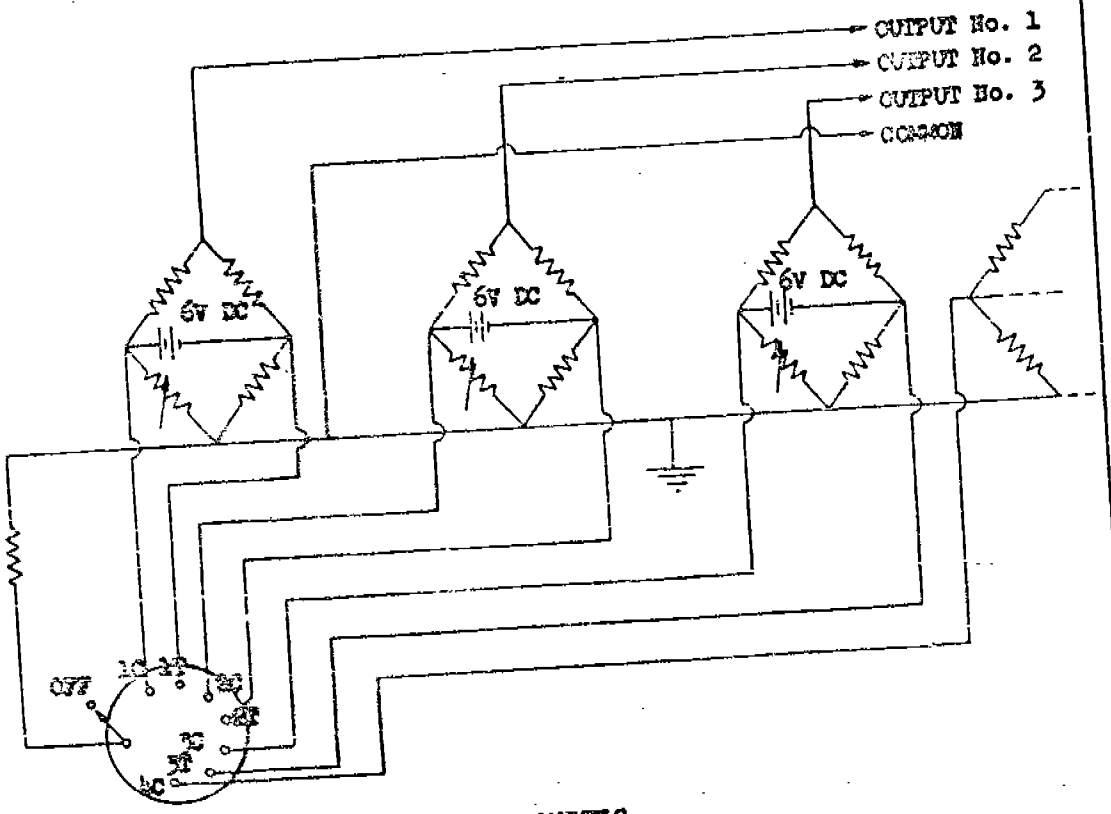

STRAIN CHANNELS

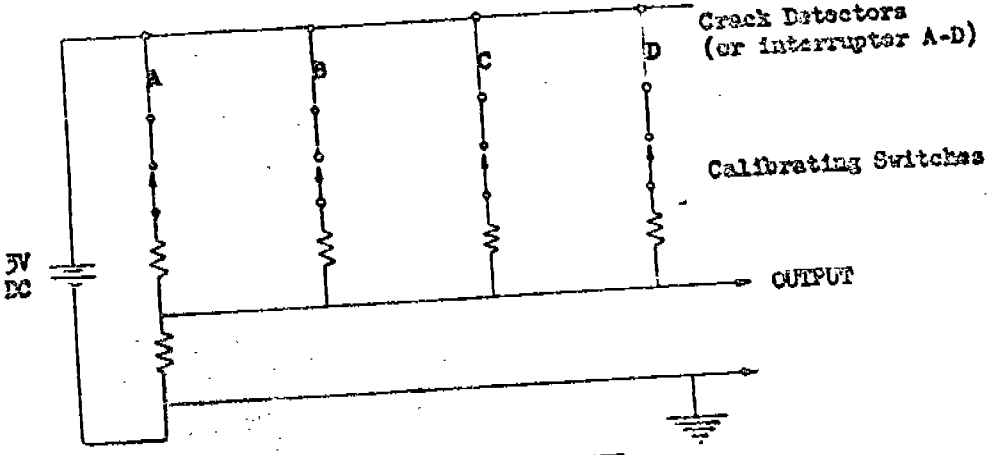

CRACK SPEED DETECTOR CIRCUIT

FIG. 28 INPUT CIRCUITS

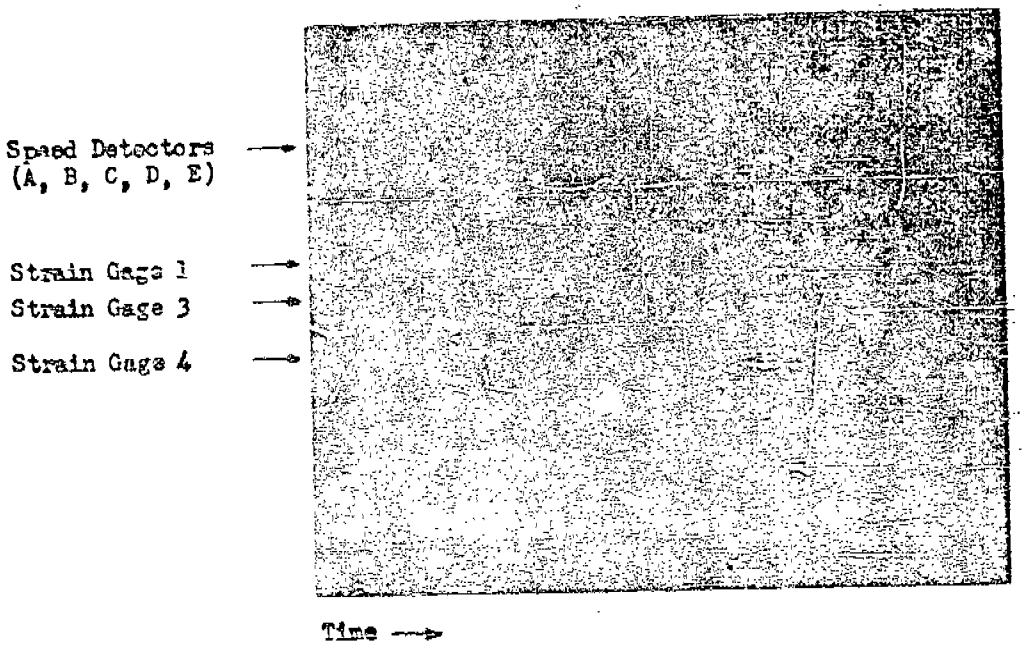

Record — Test 10

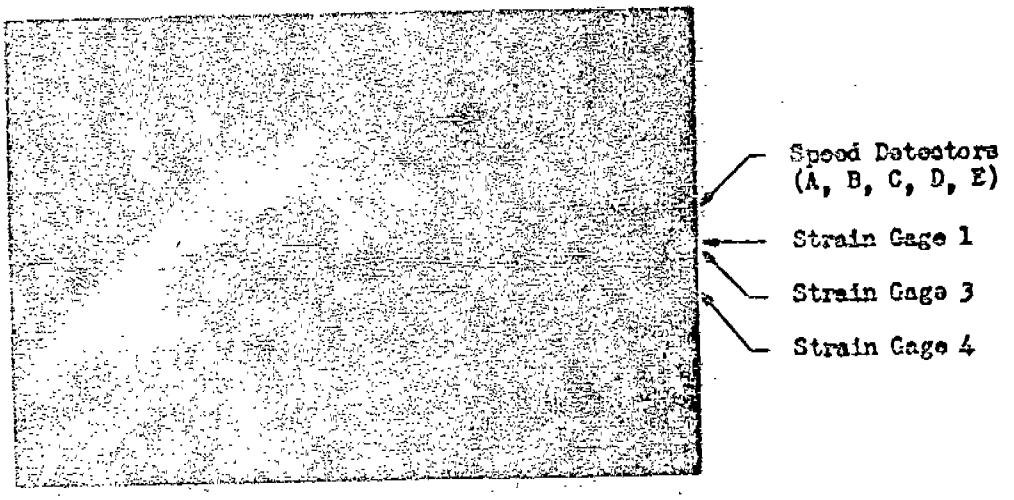

Calibration as Recorded by DuMont Oscilloscope

FIG. 29 TYPICAL TEST RECORD AND CALIBRATION — TEST 10

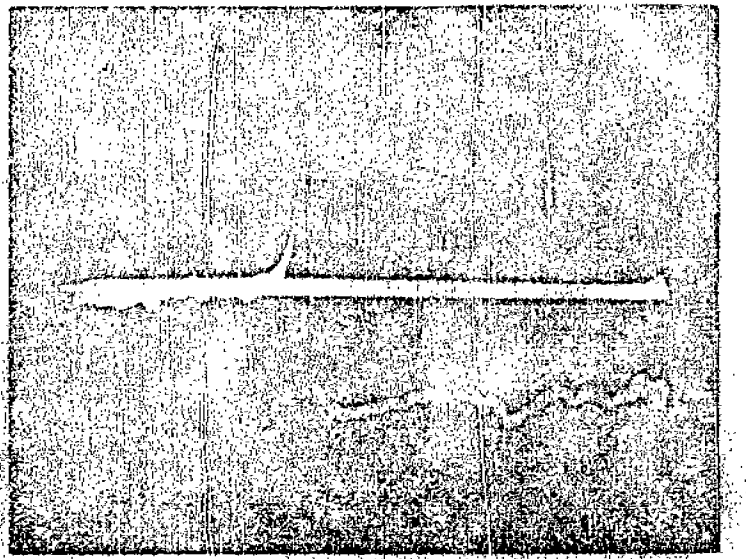

Time →

Record of Gage 3 — Test 9

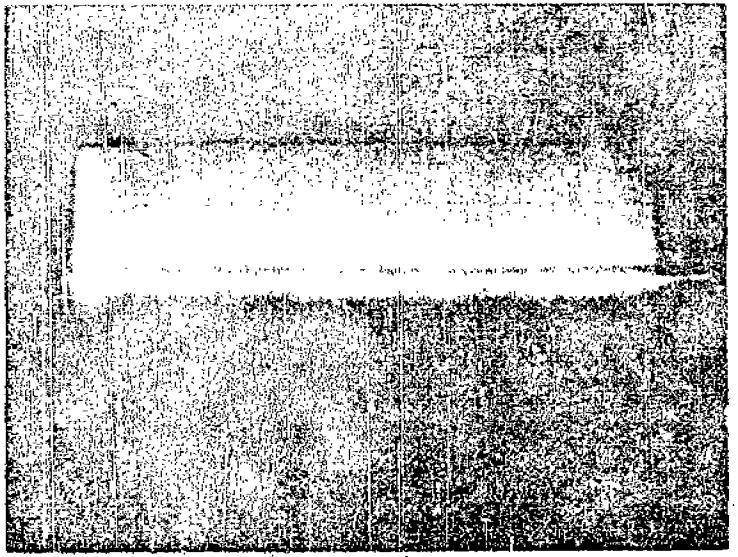

Time →

Calibration as Recorded on Tektronix Oscilloscope

Tektronix Strain-Time Response
(Calibration Switch closed at t_0)

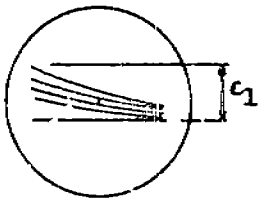

Sketch of Tektronix Calibration

FIG. 30 TYPICAL TEST RECORD AND CALIBRATION — TEST 9

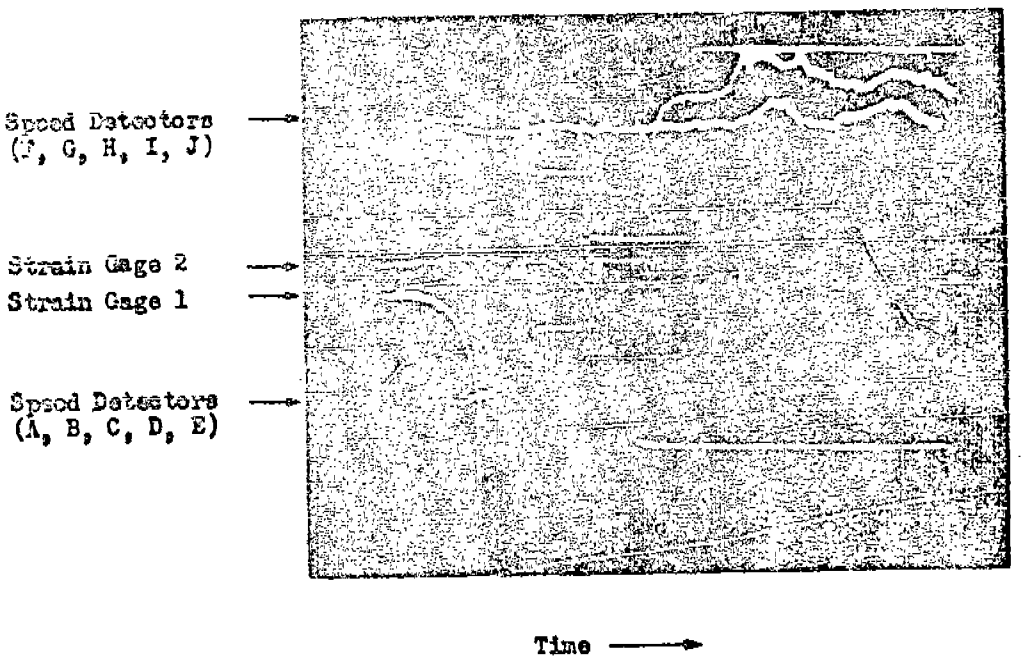

FIG. 31 DYNAMIC STRAIN-TIME-RECORD — TEST 1

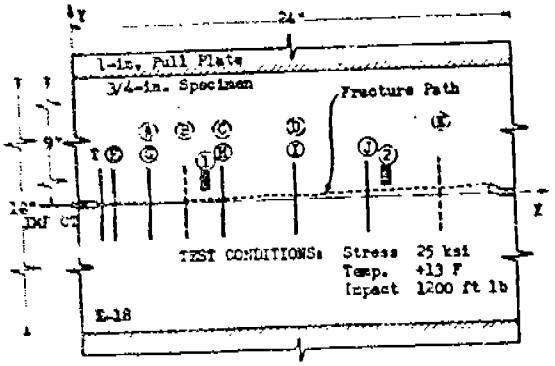

A-7 STRAIN GAGES					DETECTORS		DETECTORS	
No.	Orientation	X in.	Y in.	Y_{a-c} in.	No.	X in.	No.	X in.
1.	V	+7.0	+1.25	+1.0	A	+4.0	F	+2.0
2.	V	+17.0	+1.25	+0.8	B	+6.0	G	+4.0
					C	+8.0	H	-3.0
					D	-12.0	I	+12.0
					E	+20.0	J	+16.0

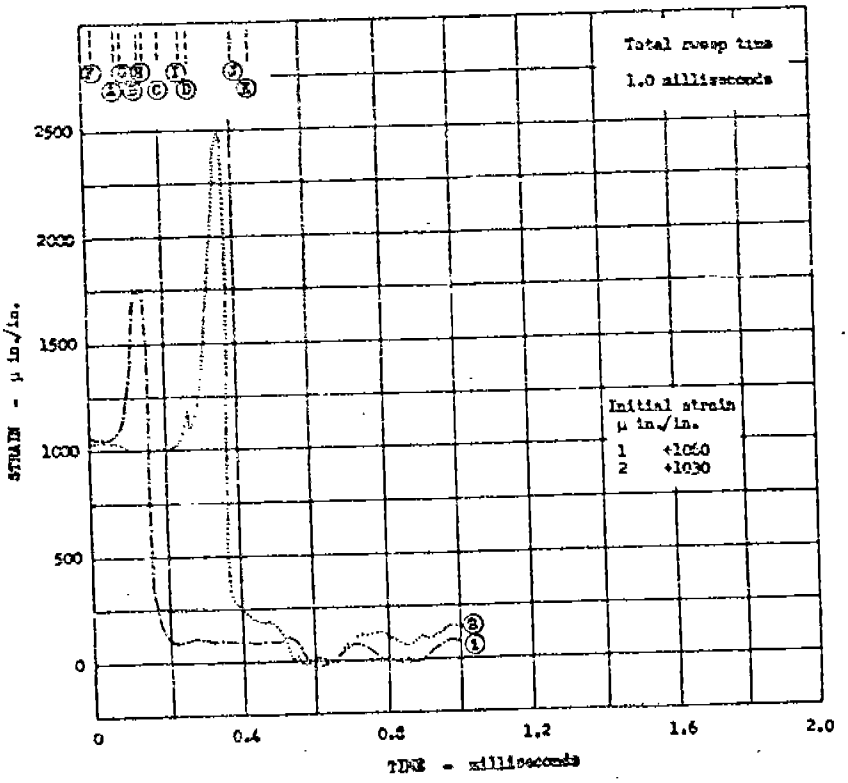

FIG. 32 SCALED RECORD AND INSTRUMENTATION -- TEST 1

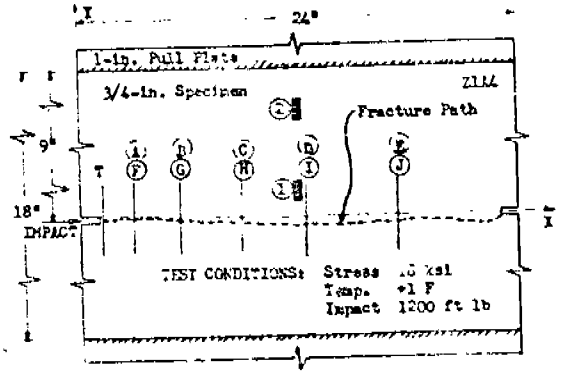

A-7 STRAIN GAGES					DETECTORS		DETECTORS	
No.	Orientation	X in.	Y in.	$Y_{in.}^{-3}$	No.	X in.	No.	X in.
1.	V	+12.0	+1.5	+1.7	A	+3.0	F	+3.0
2.	V	+12.0	+6.0	+6.2	B	+5.5	G	+5.5
					C	+9.0	H	+9.0
					D	+12.5	I	+12.5
					E	+17.5	J	+17.5

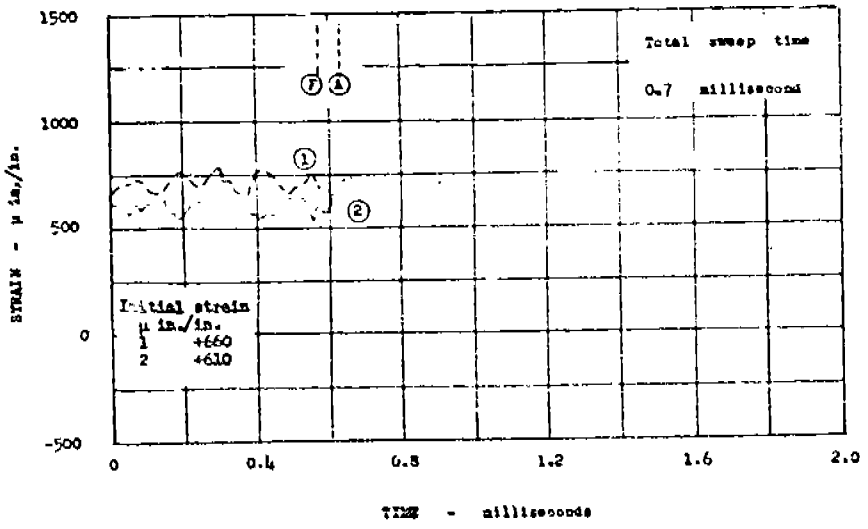

FIG. 33 SCALED RECORD AND INSTRUMENTATION -- TEST 5

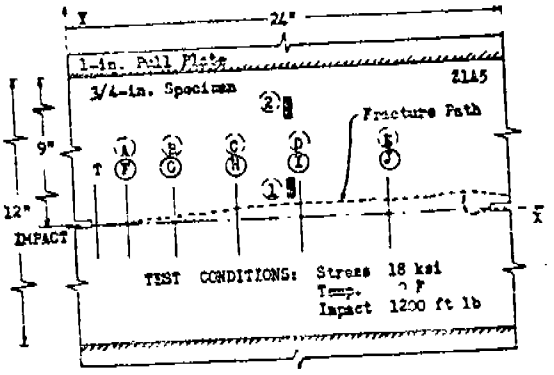

A-7 STRAIN GAGES					DETECTORS		DETECTORS	
No.	Orientation	X in.	Y in.	Y_c in.	No.	X in.	No.	X in.
1.	Y	+12.0	+1.5	+0.9	A	+3.0	F	+3.0
2.	Y	+12.0	-6.0	+5.4	B	+5.5	G	+5.5
					C	+9.0	H	+9.0
					D	+12.5	I	+12.5
					E	+17.5	J	+17.5

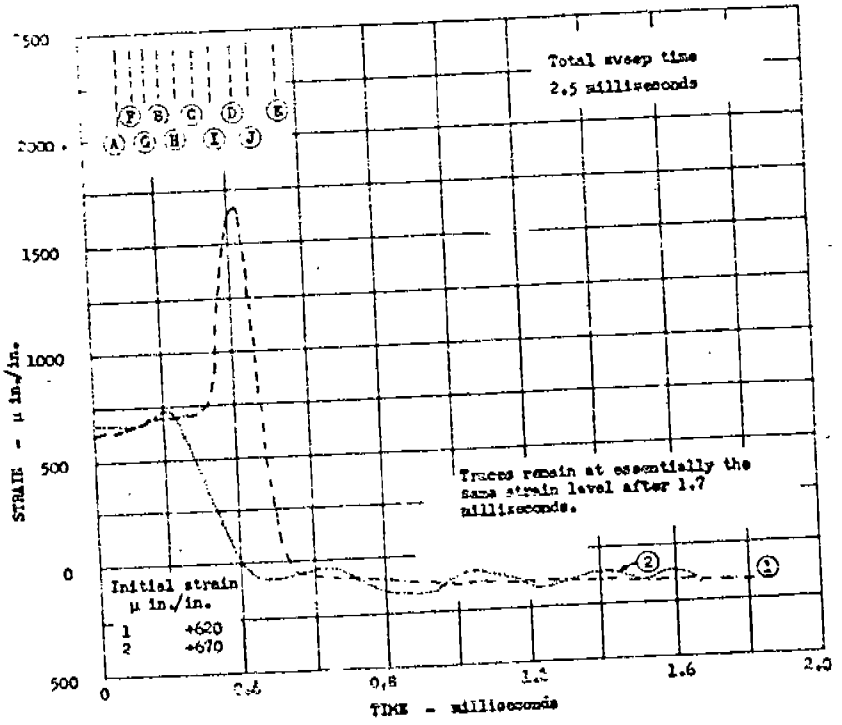

FIG. 34 SCALED RECORD AND INSTRUMENTATION — TEST 6

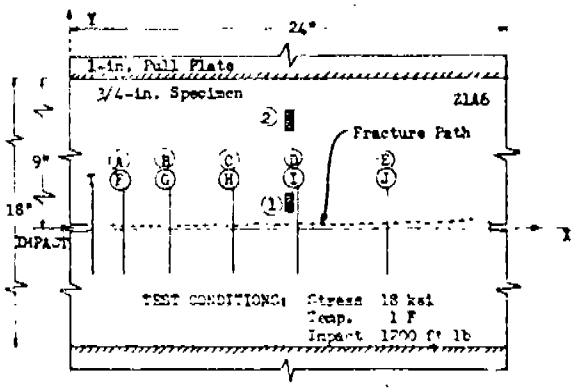

A-7 STRAIN GAGES					DETECTORS		DETECTORS	
No.	Orientation	X in.	Y in.	Y_0 in.	No.	X in.	No.	X in.
1.	V	+12.0	+1.5	+1.2	A	+3.0	F	+3.0
2.	V	+12.0	+6.0	+5.7	B	+5.5	G	+5.5
					C	+9.0	H	+9.0
					D	+12.5	I	+12.5
					E	+17.5	J	+17.5

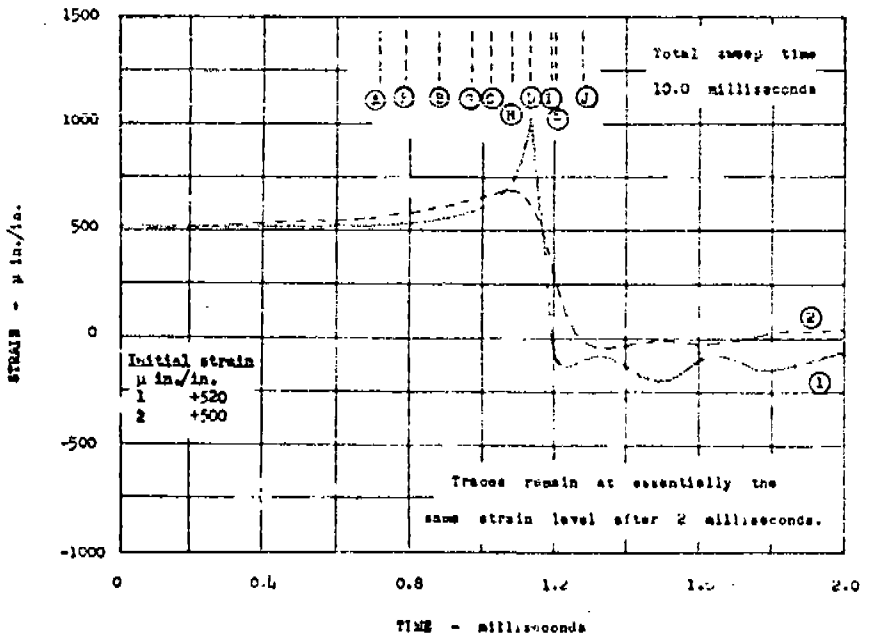

FIG. 35 SCALED RECORD AND INSTRUMENTATION — TEST 7

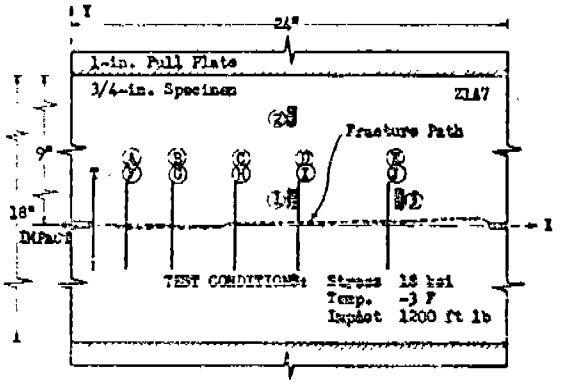

A-7 STRAIN GAGES					DETECTORS		DETECTORS	
No.	Orientation	X in.	Y in.	Y—g in.	No.	X in.	No.	X in.
1.	V	+12.0	+1.5	+1.5	A	+3.0	F	+3.0
2.	V	+12.0	+6.0	+6.0	B	+5.5	G	+5.5
3.	V	+18.0	+1.5	+1.2"	C	+9.0	H	+9.0
					D	+12.5	I	+12.5
					E	+17.5	J	+17.5

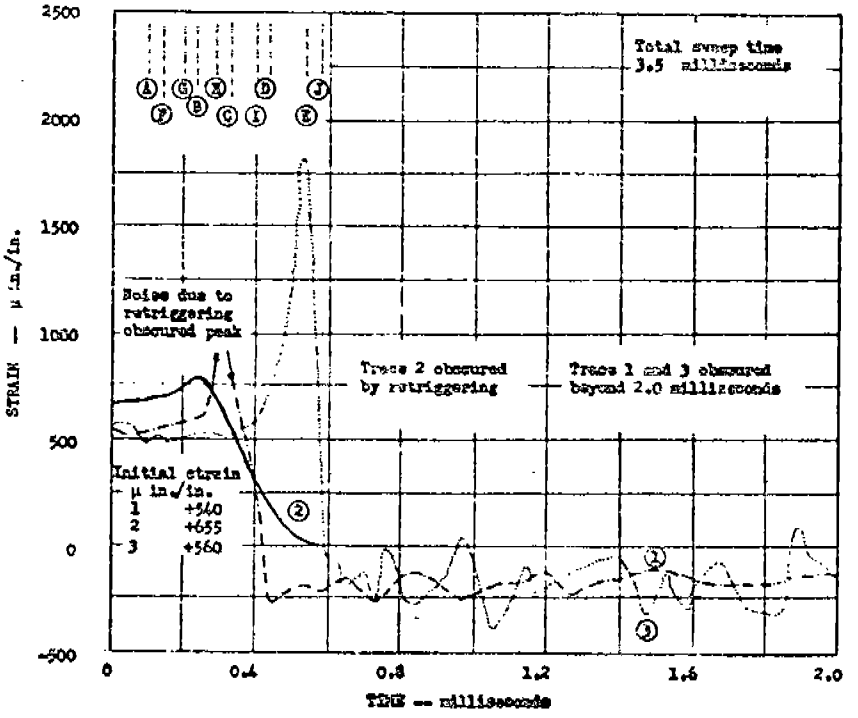

FIG. 36 SCALED MED [illegible] AND INSTRUMENTATION — TEST 9

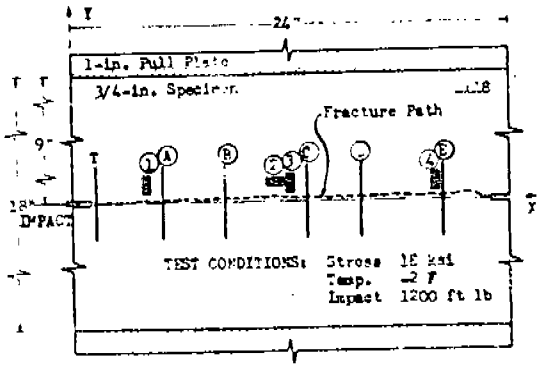

A-7 STRAIN GAGES					DETECTORS	
No.	Orientation	X in.	Y in.	Y_{p-p} in.	No.	X in.
1.	V	+4.0	-1.0	+1.0	A	+5.0
2.	H	+11.25	+1.0	+0.8	B	+8.5
3.	V	+12.0	+1.0	+0.8	C	+13.0
4.	V	+20.0	+1.0	+0.7	D	+16.0
					E	+20.5

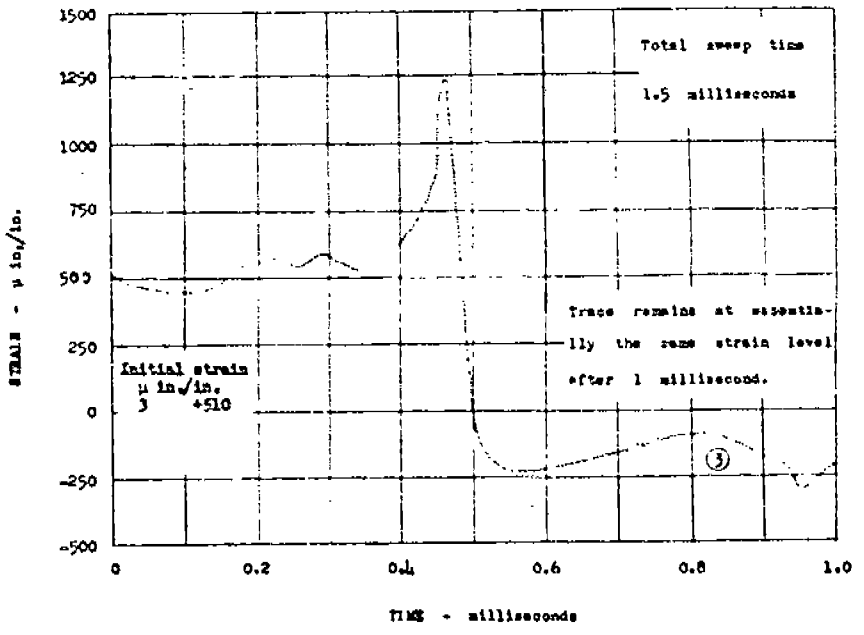

FIG. 37 SCALED RECORD AND INSTRUMENTATION — TEST 9

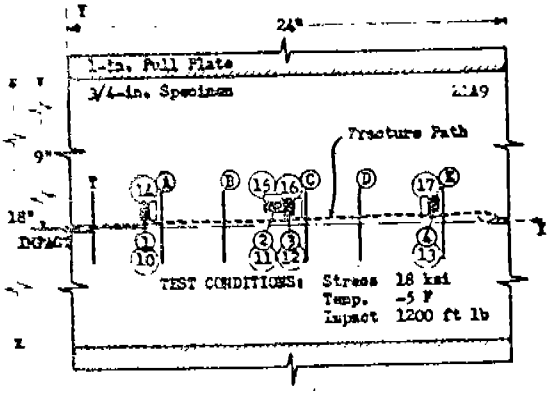

A-7 STRAIN GAGES					A-7 STRAIN GAGES					LOCATIONS	
No.	Orientation	X in.	Y in.	Y_{0-1} in.	No.	Orientation	X in.	Y in.	Y_{2-3} in.	No.	X in.
1.	Y	-4.0	+1.0	+0.8	12.	Y	+12.0	+1.0	+0.7	A	-5.0
2.	X	+11.25	+1.0	+0.7	13.	Y	+20.0	+1.0	+0.6	B	+8.5
3.	Y	+12.0	+1.0	+0.7	14.	Y	-4.5	+1.0	+0.8	C	+13.0
4.	Y	+20.0	+1.0	+0.6	15.	X	+11.25	+1.5	+1.2	D	+16.0
10.	Y	-4.0	-1.0	+0.8	16.	Y	+12.5	+1.0	+0.7	E	+20.5
11.	X	+11.25	+1.0	+0.7	17.	Y	+19.5	+1.0	+0.6		

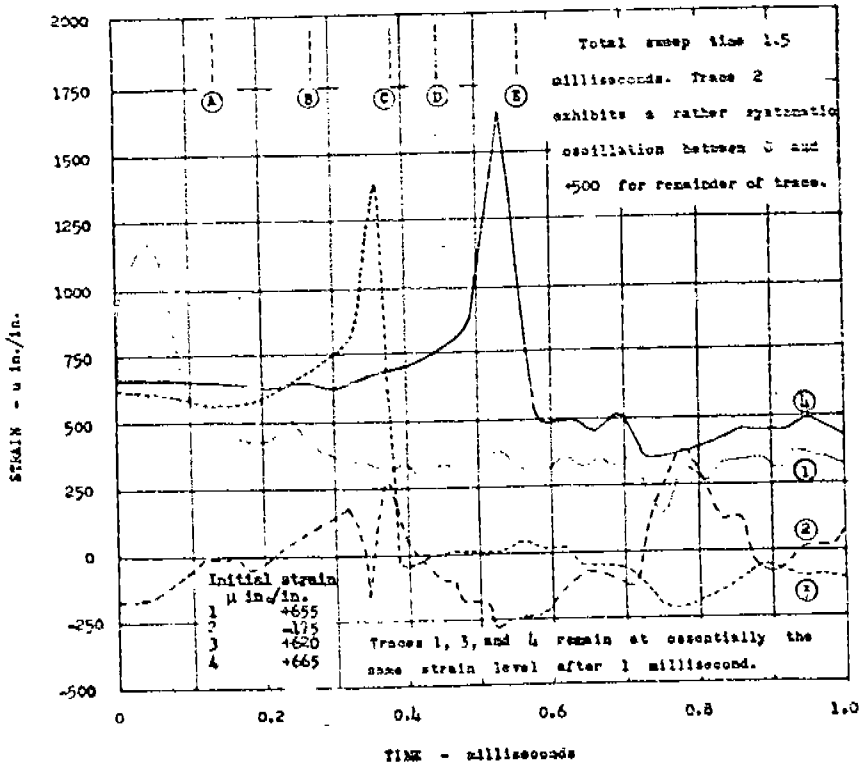

FIG. 38 SCALED RECORD AND INSTRUMENTATION — TEST 10

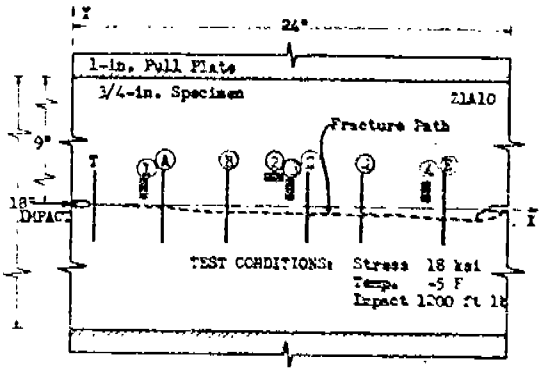

A-7 STRAIN GAGES					DETECTORS	
No.	Orientation	X in.	Y in.	[illegible] in.	No.	X in.
1.	V	-4.0	-1.0	+1.1	A	+5.0
2.	H	+11.25	+1.5	+1.9	B	+8.5
3.	V	+12.0	-1.0	+1.4	C	+13.0
4.	V	+19.5	+1.0	+1.6	D	+16.0
					E	+20.5

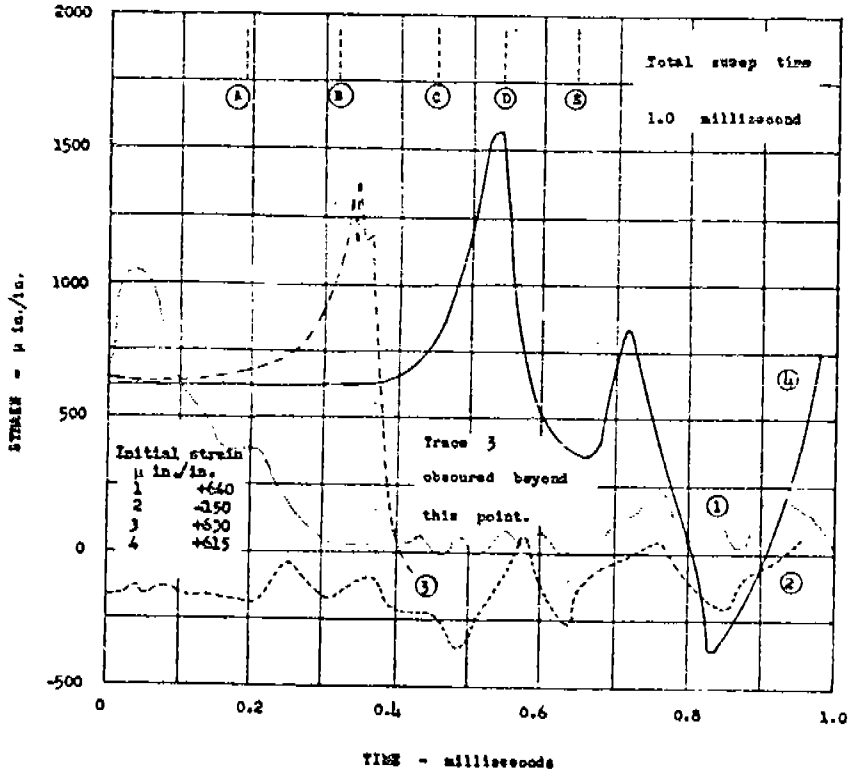

FIG. 39 SCALED RECORD AND INSTRUMENTATION -- TEST 11

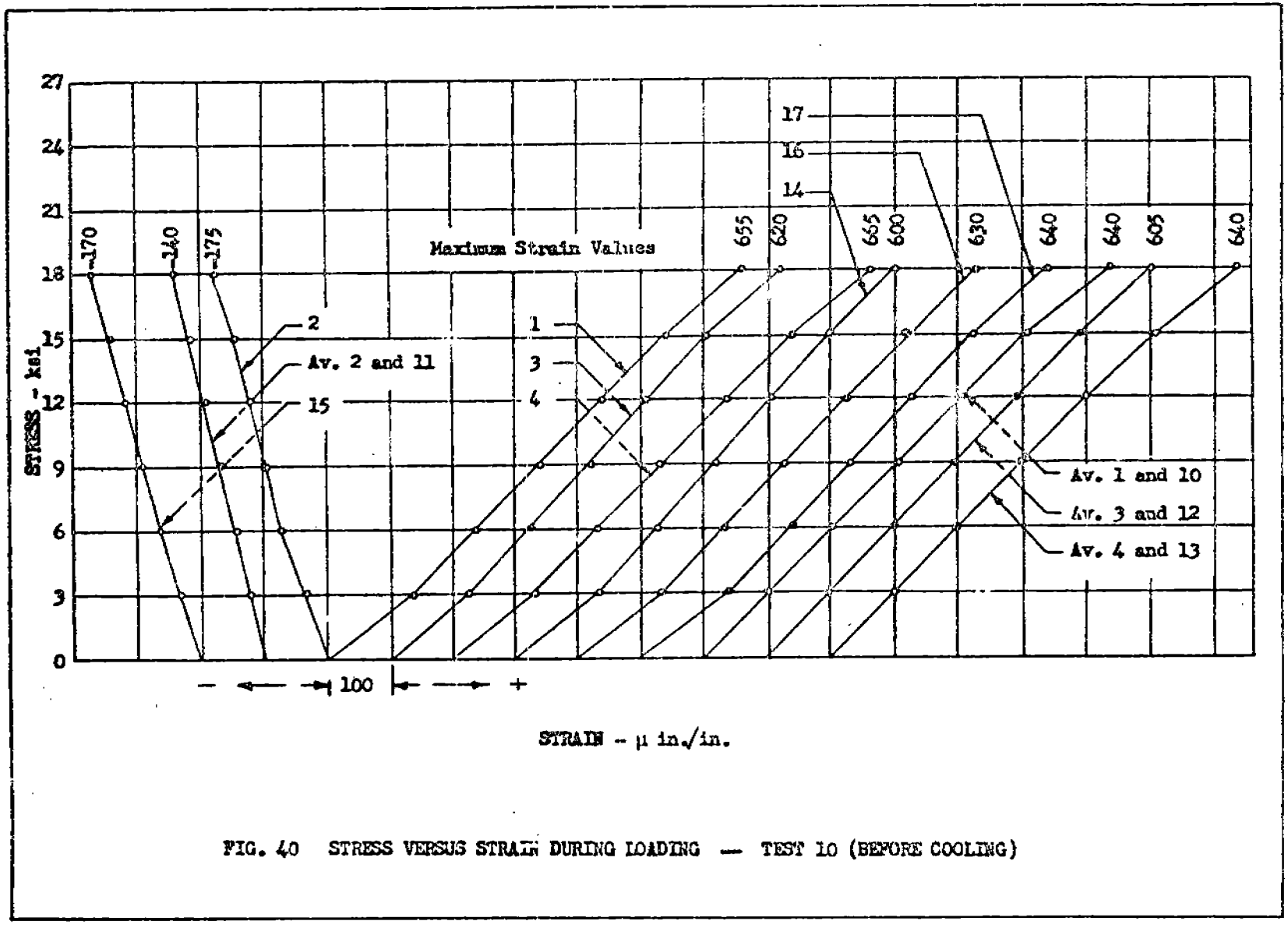

FIG. 40 STRESS VERSUS STRAIN DURING LOADING — TEST 10 (BEFORE COOLING)

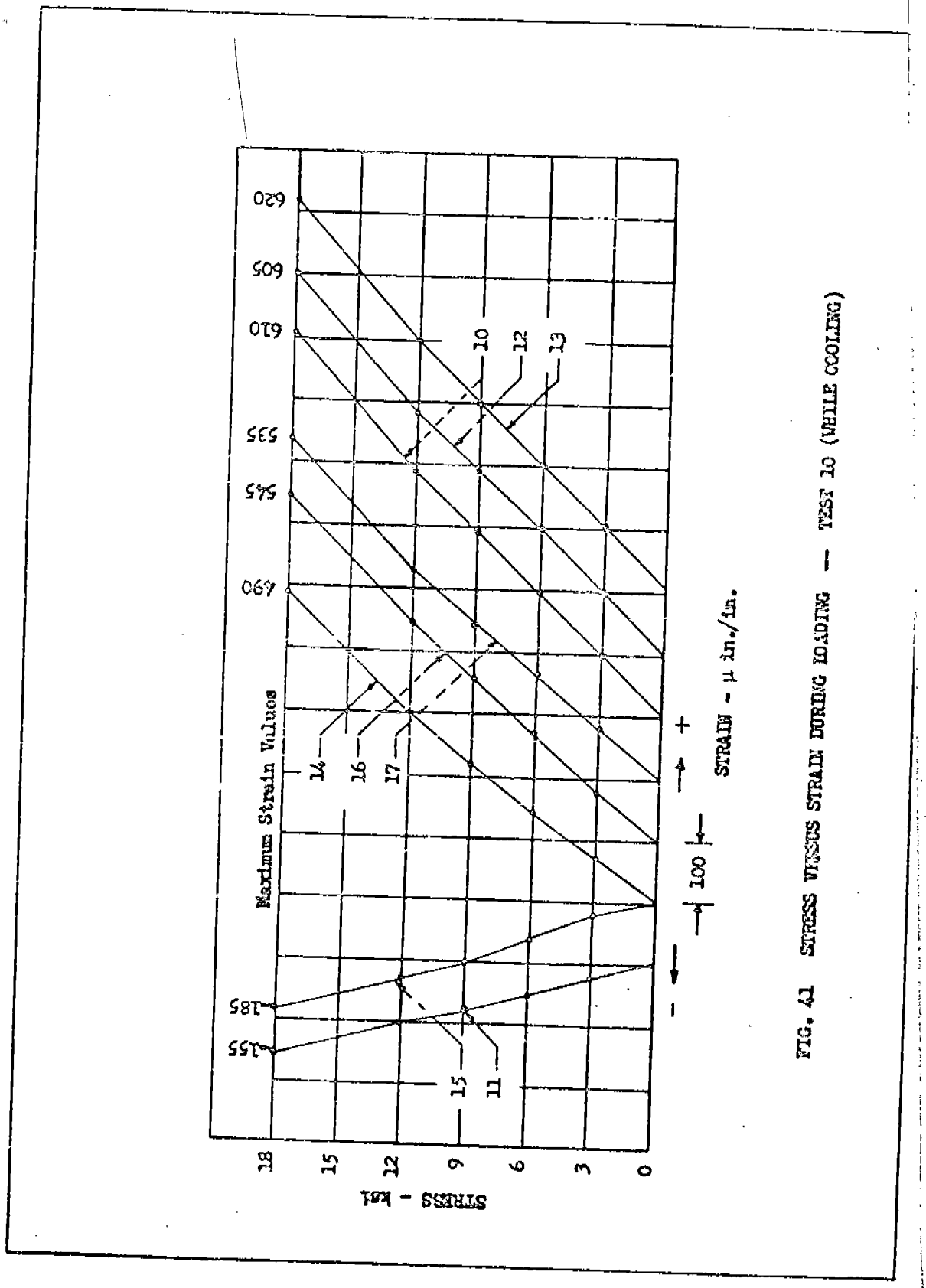

FIG. 41 STRESS VERSUS STRAIN DURING LOADING — TEST 10 (WHILE COOLING)

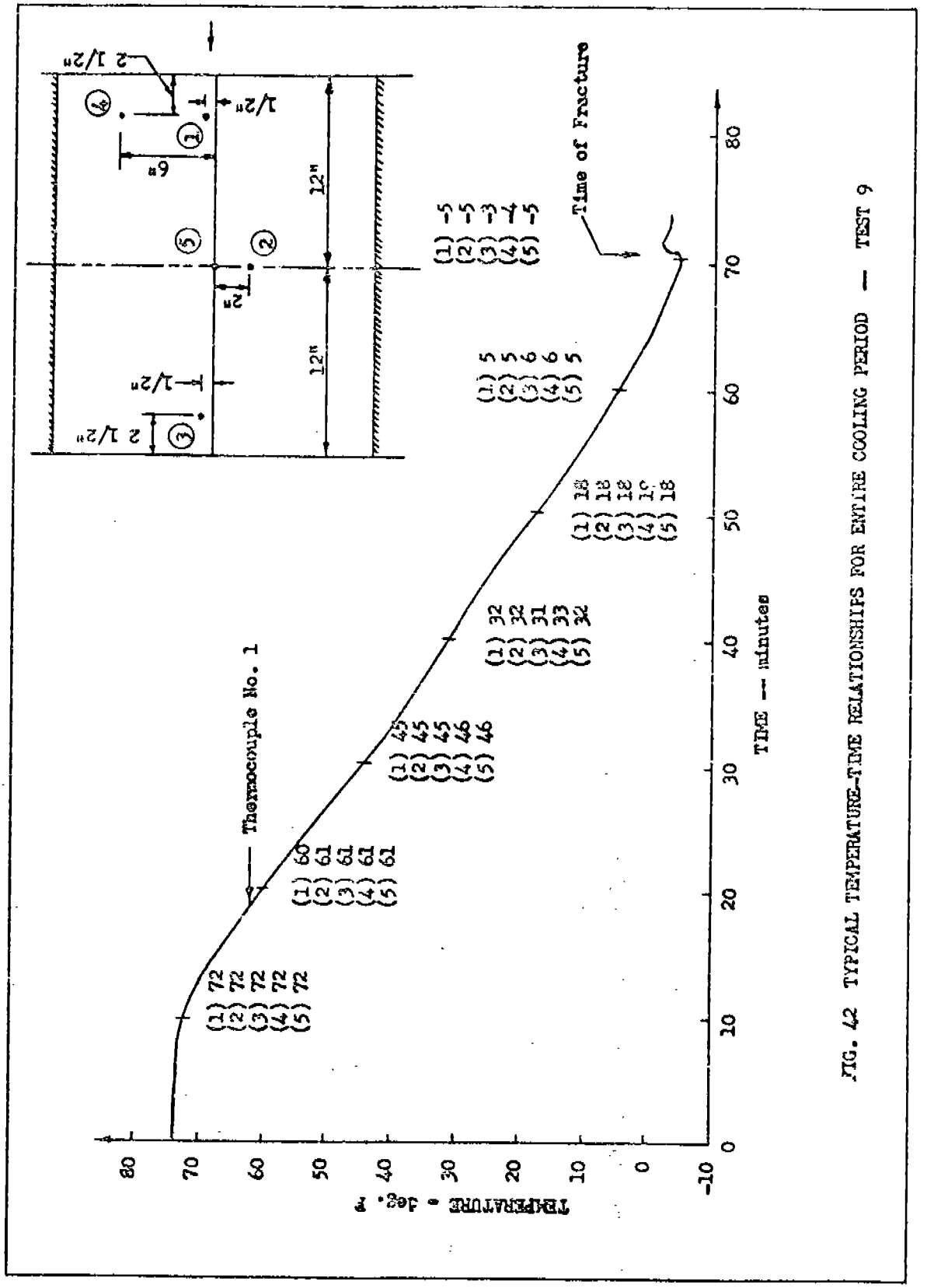

FIG. 42 TYPICAL TEMPERATURE-TIME RELATIONSHIPS FOR ENTIRE COOLING PERIOD — TEST 9

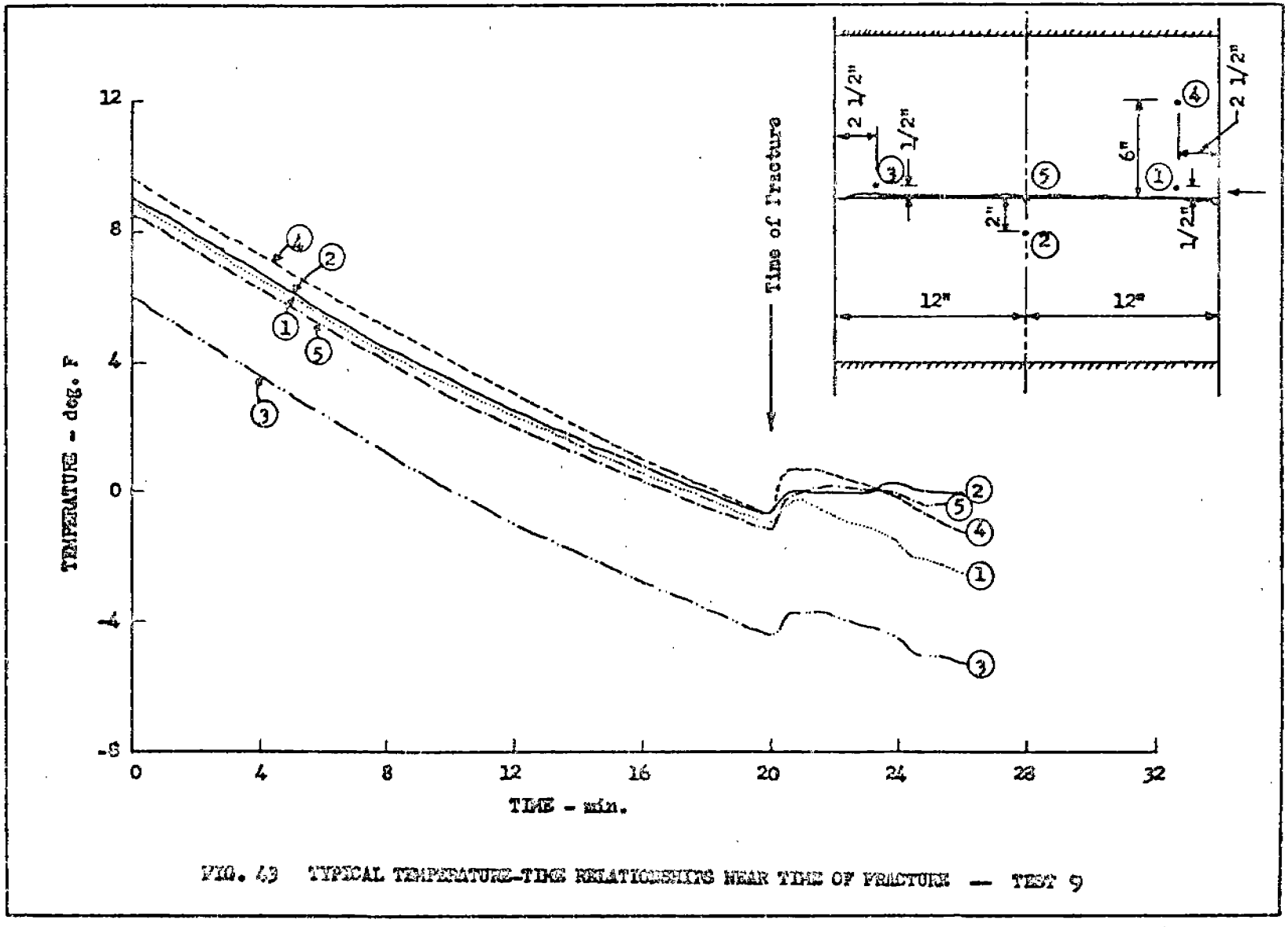

FIG. 43 TYPICAL TEMPERATURE-TIME RELATIONSHIPS NEAR TIME OF FRACTURE — TEST 9

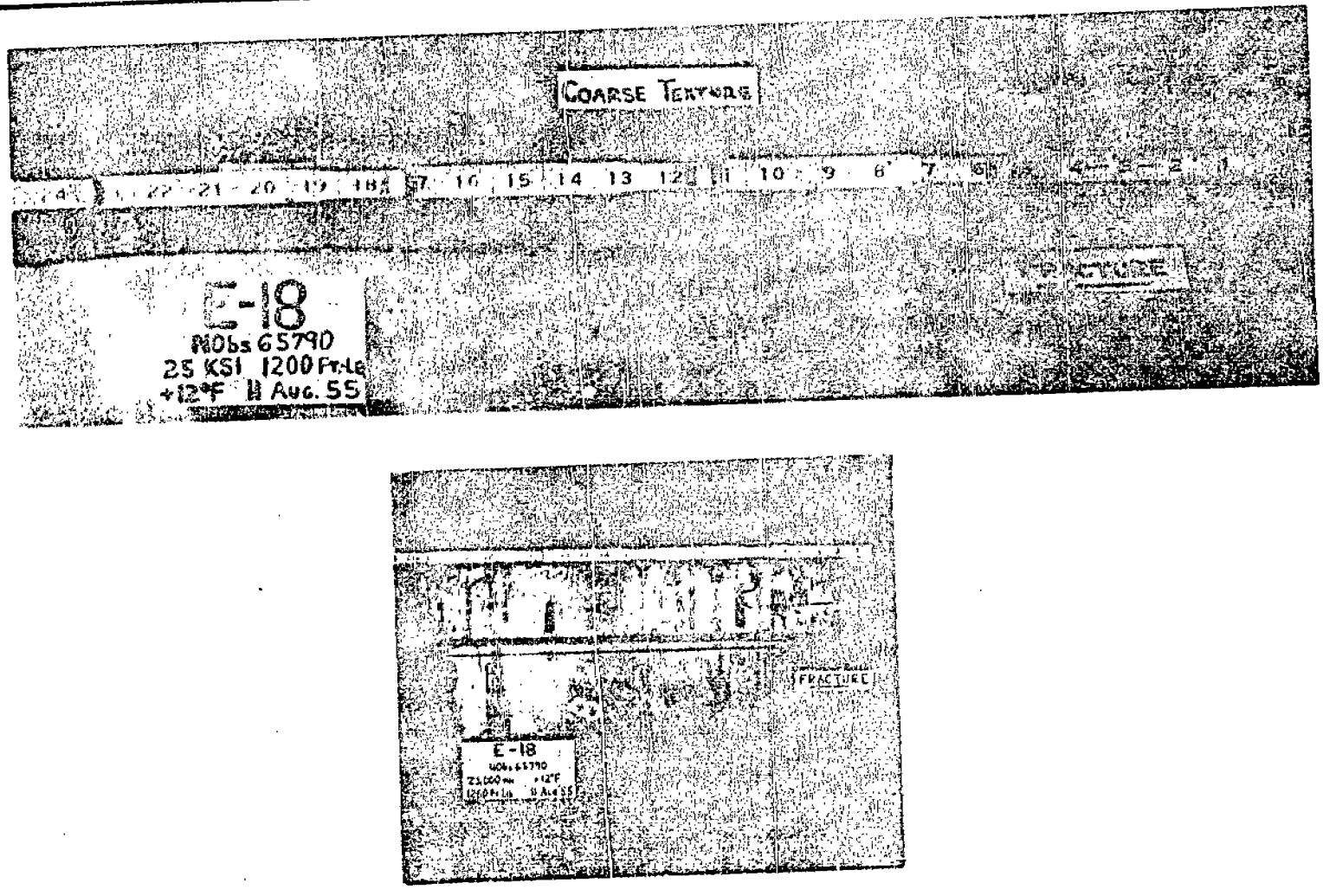

FIG. 44 FRACTURE SURFACE AND PATH — TEST 1

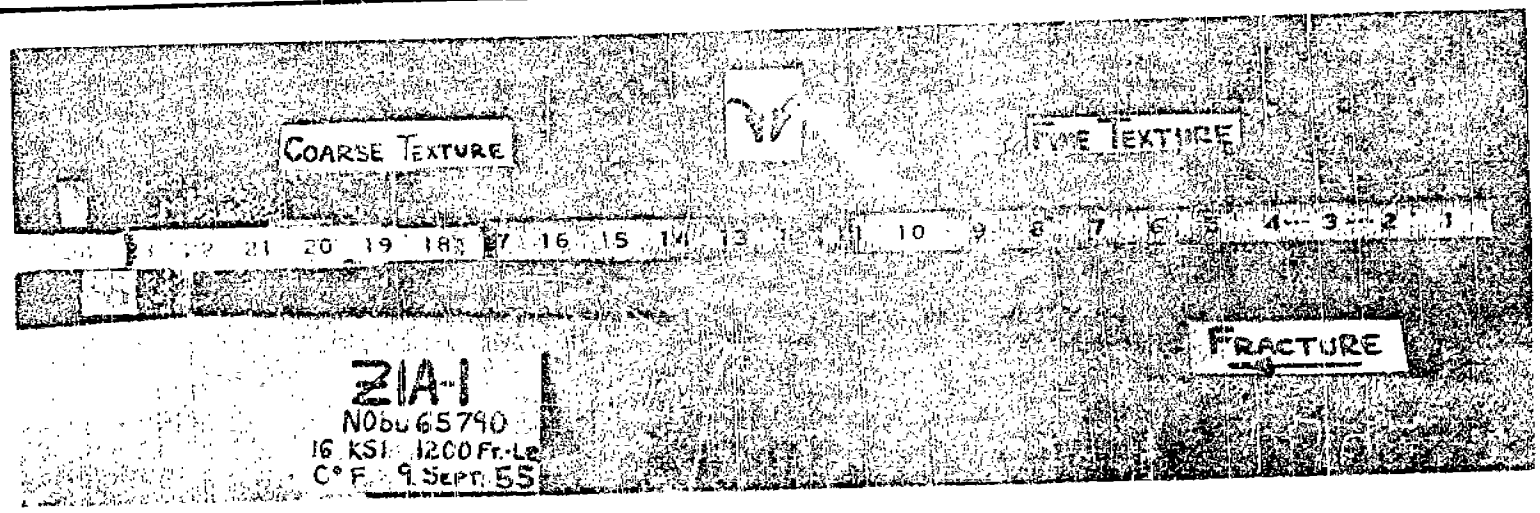

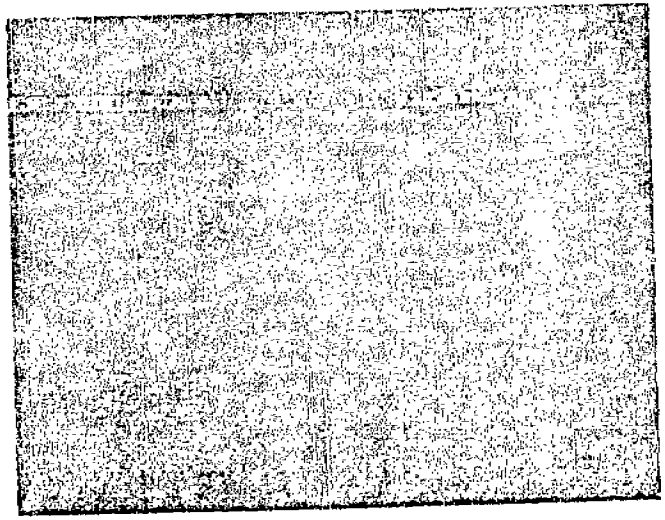

FIG. 45 FRACTURE SURFACE AND PATH — TEST 2

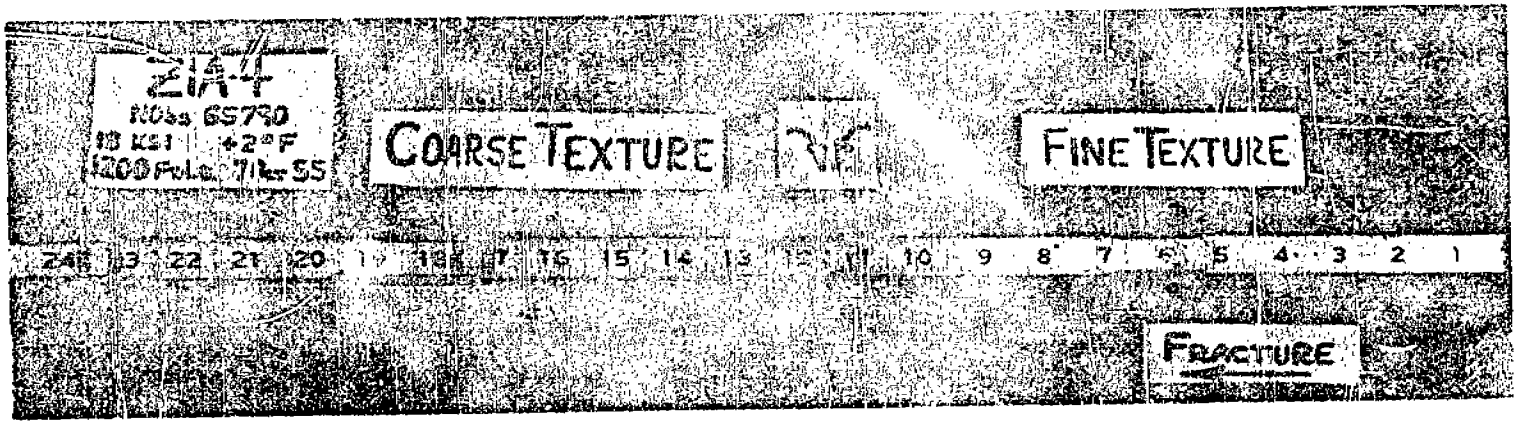

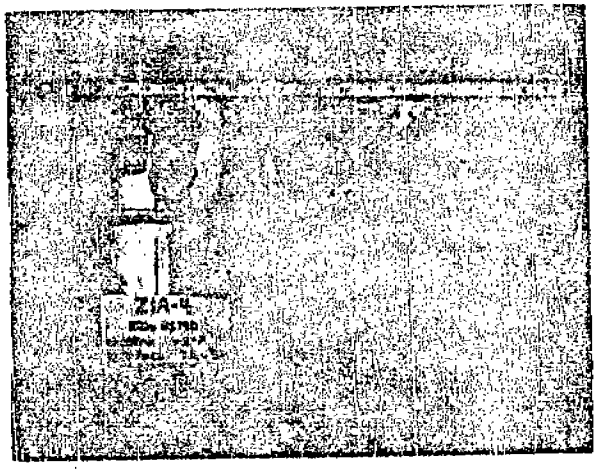

FIG. 46 FRACTURE SURFACE AND PATH — TEST 5

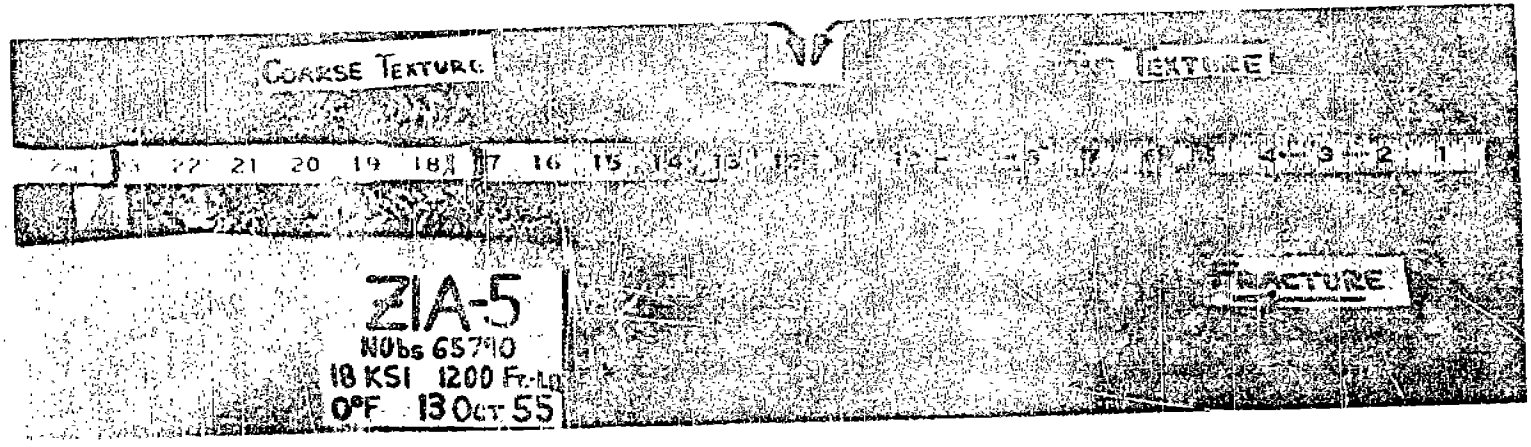

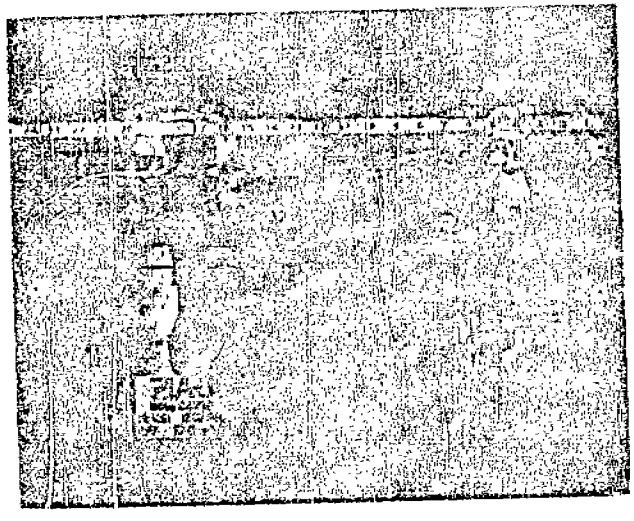

FIG. 47 FRACTURE SURFACE AND PATH—TEST 6

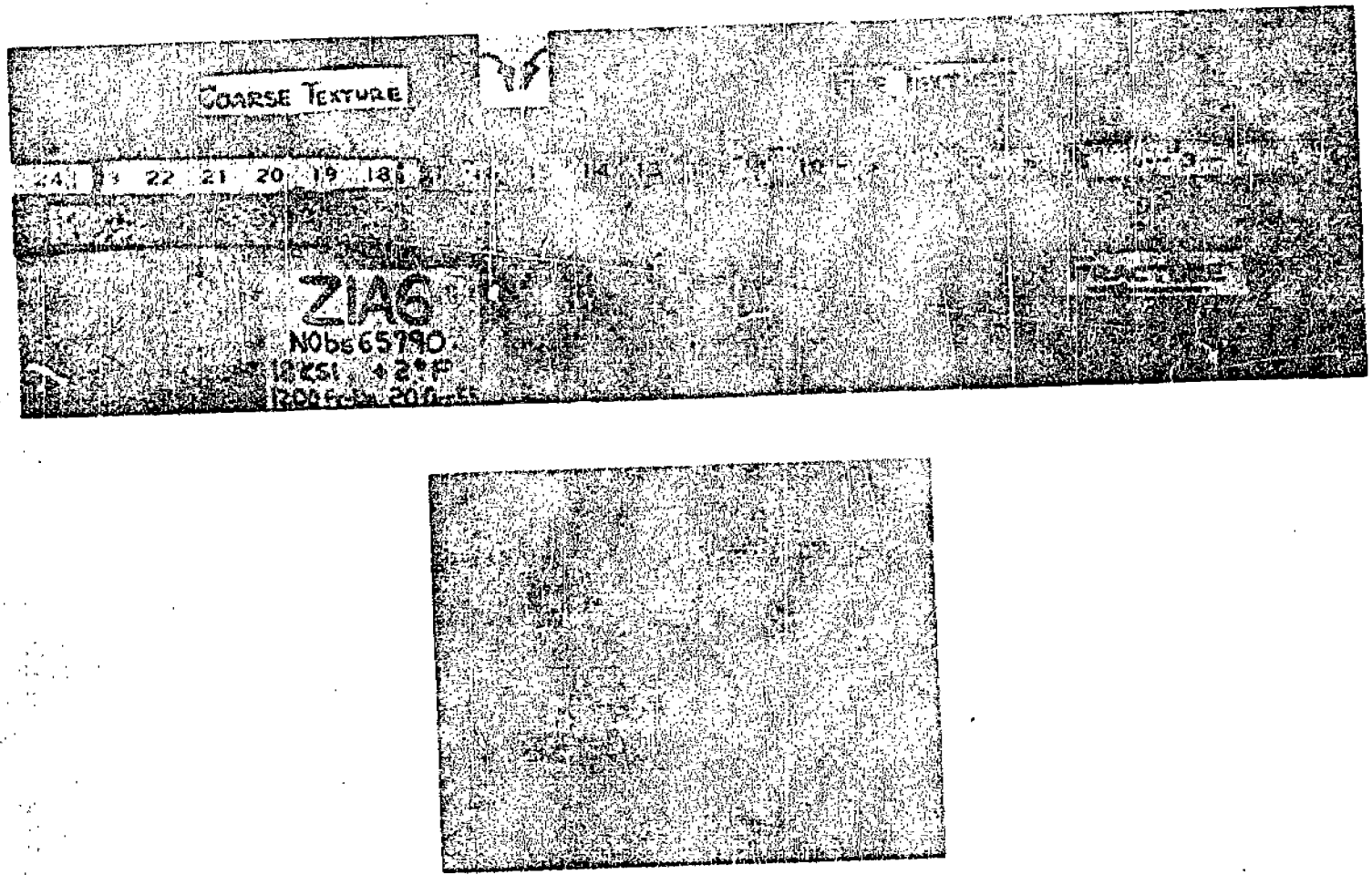

FIG. 48 FRACTURE SURFACE AND PATH — TEST 7

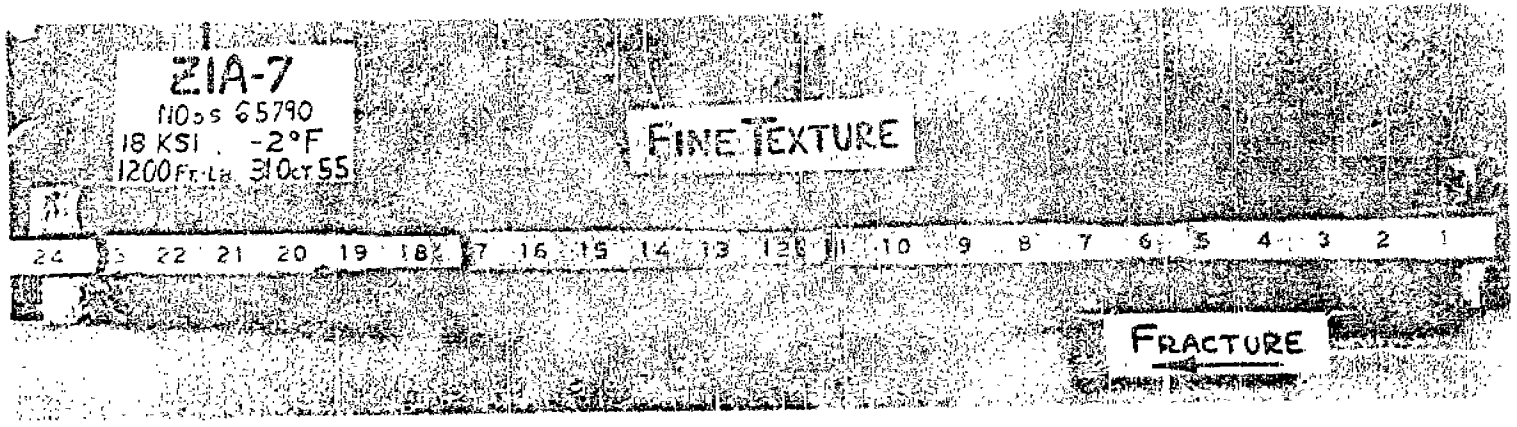

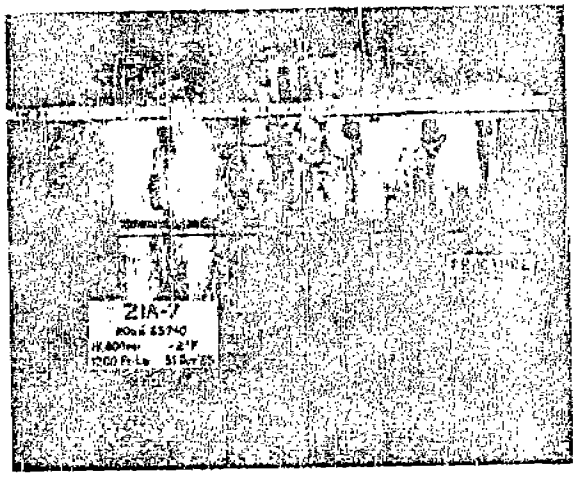

FIG. 49 FRACTURE SURFACE AND PATH — TEST 8

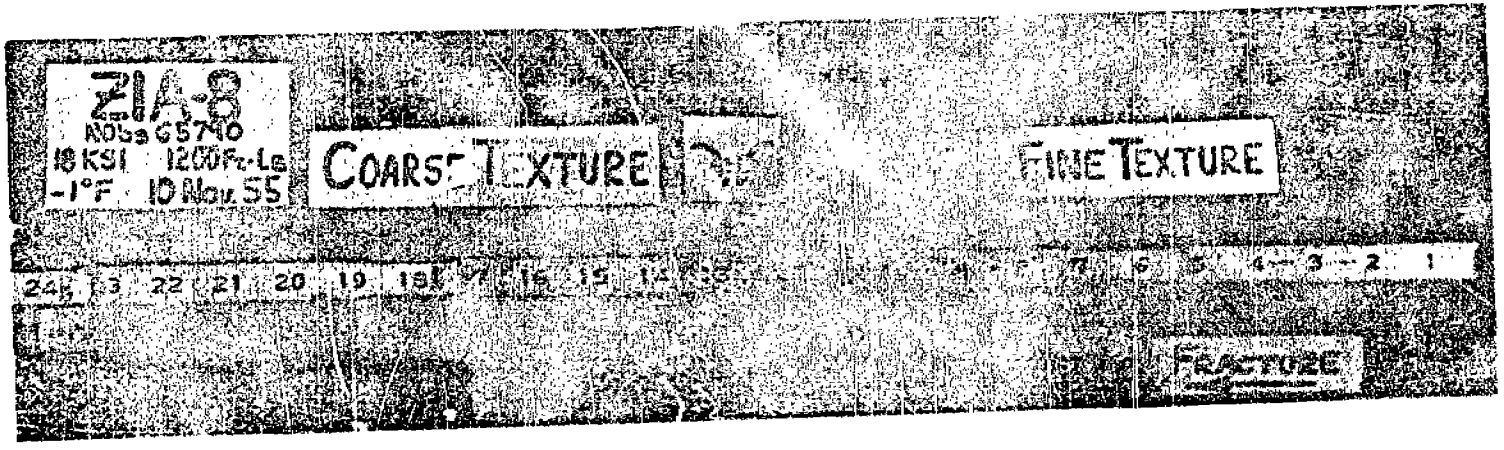

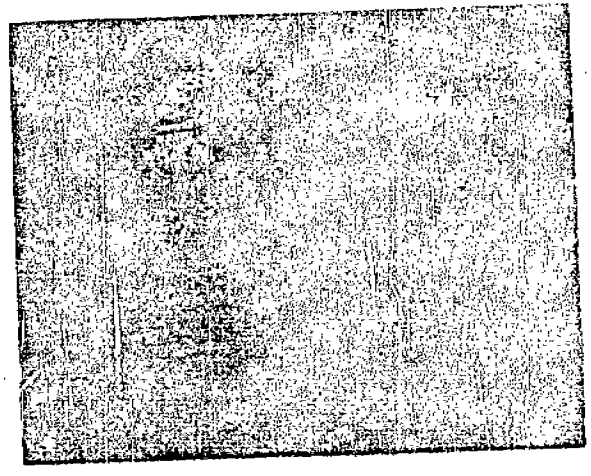

FIG. 50 FRACTURE SURFACE AND PATH — TEST 9

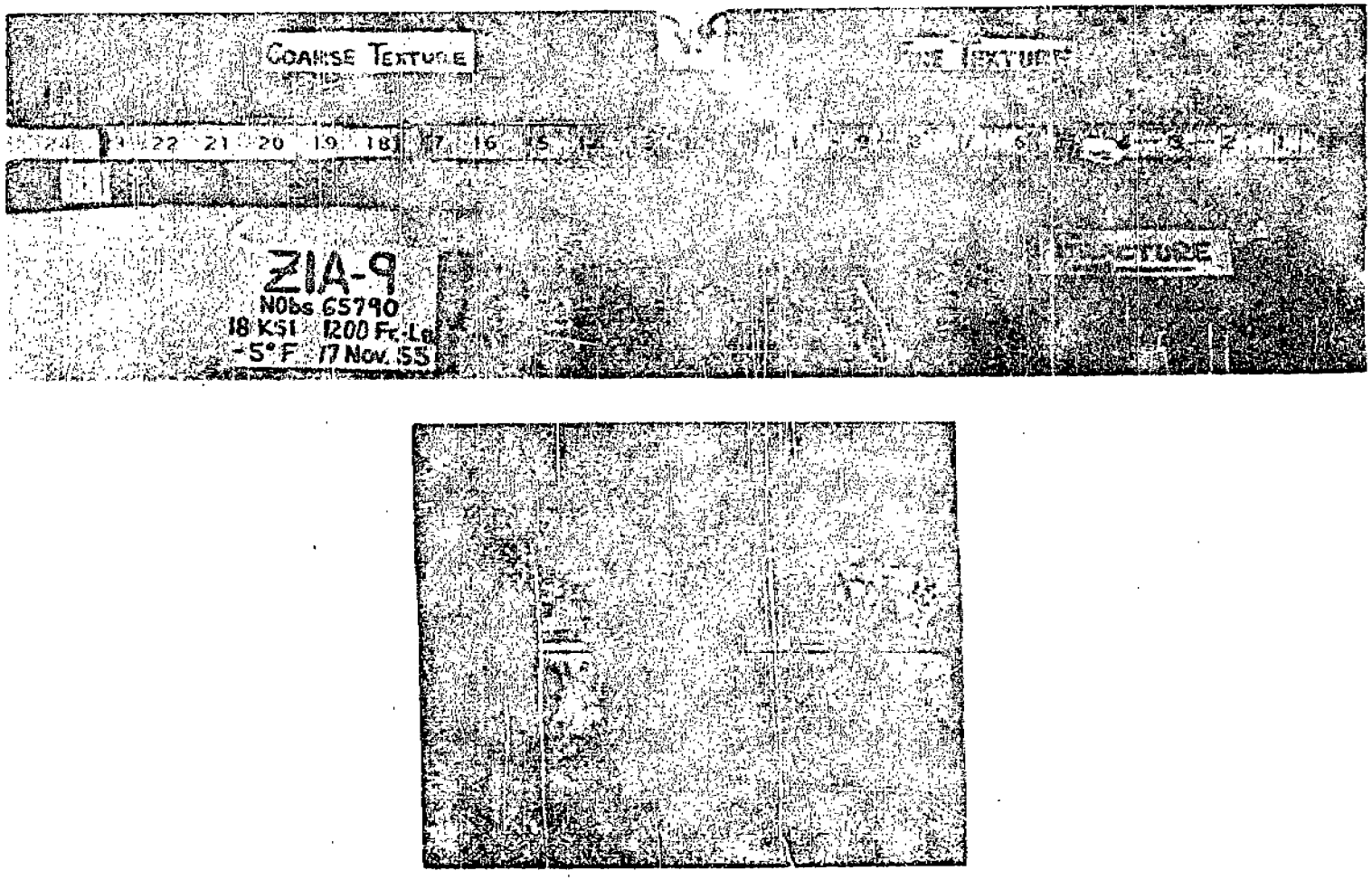

FIG. 51 FRACTURE SURFACE AND PATH — TEST 10

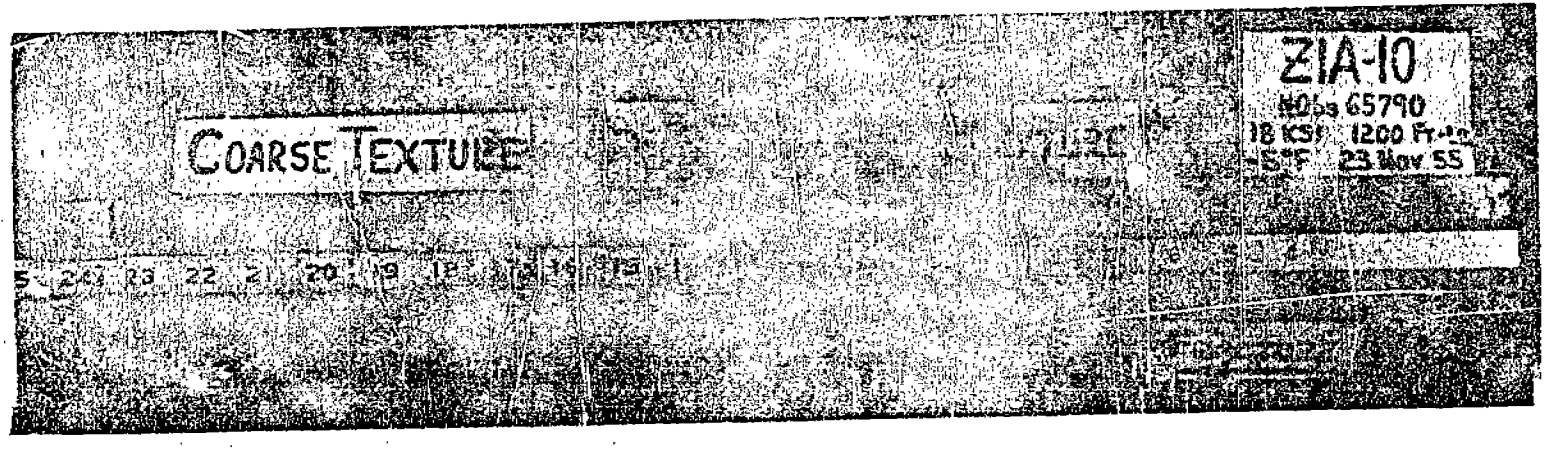

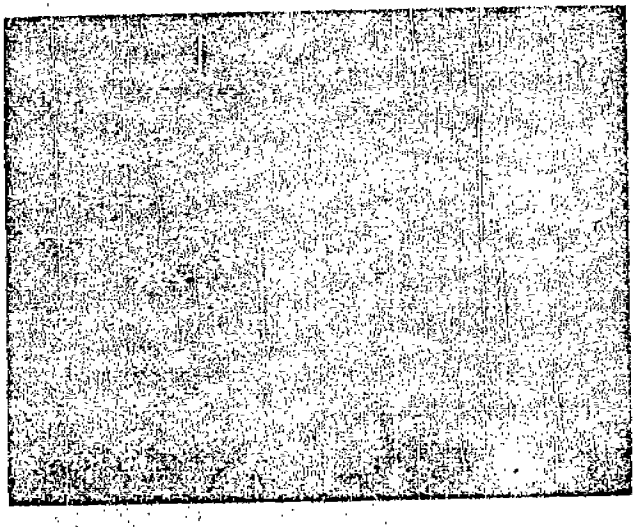

FIG. 52 FRACTURE SURFACE AND PATH — TEST II

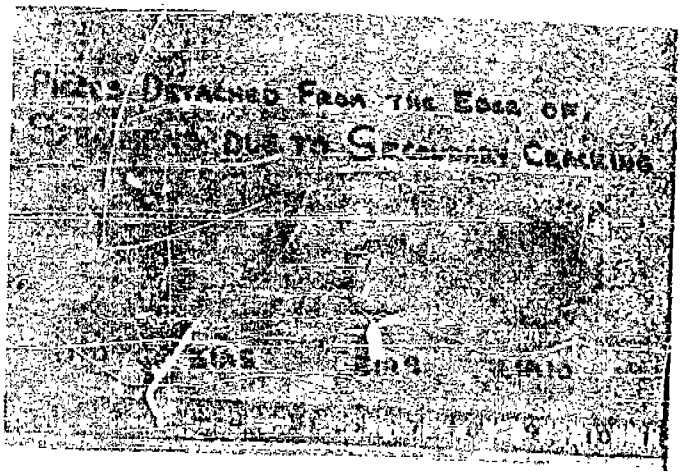

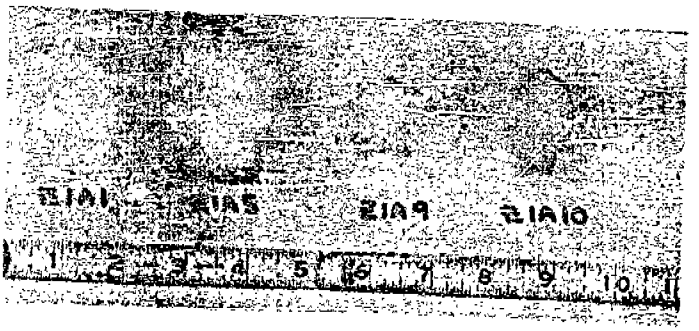

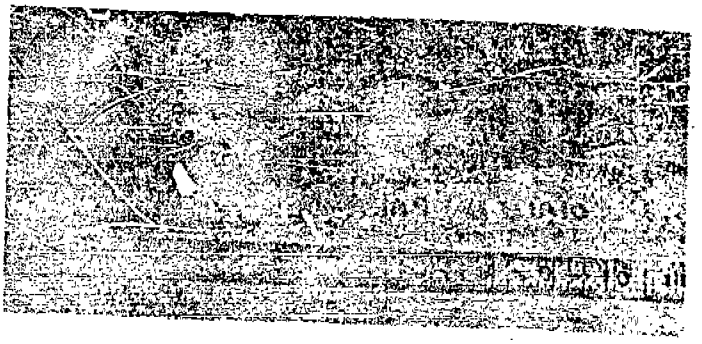

FIG. 53 PIECES DETACHED FROM EDGE OF SPECIMEN BY SECONDARY CRACK (FROM LEFT TO RIGHT, TESTS 2, 6, 10, 11)

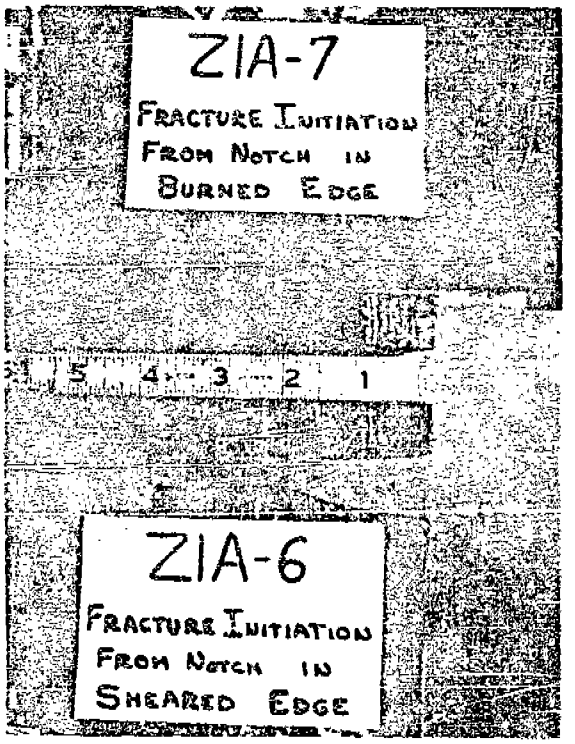

FIG. 54 TYPICAL FRACTURE INITIATION REGIONS — SHEARED EDGE (SPECIMEN Z1A6 - TEST 7) AND BURNED EDGE (SPECIMEN Z1A7 - TEST 8)